People's Democratic Republic of Algeria

Ministry of Higher Education and Scientific Research

Faculty of Science and Technology

Department of Mechanical Engineering

Ref: 2020/2021

MASTER'S DISSERTATION

Option:

Materials Engineering

Synthesis and characterization of copper doped nickel oxide thin films by spray pyrolysis technique

Presented by:

SALMI Afef

Jury:

HANNACHI M.Eltaher	MCB	Tebessa University	President
DIHA Abdallah	MCA	Tebessa University	Supervisor
BOULEDROUA Basma	MAA	Tebessa University	Examiner

University year: 2020 / 2021

Dedication

I dedicate this modest work, with all my love and respect, to

My dear parents: Brahim and MOKADEM Laarem, for everything

My big sister bassma and my five brothers Ala, Bilel, Aymen, Zika, and Adem,

To all my cousins, and family,

To all my friends,

To my supervisor Dr A. DIHA,

All my post-graduate teachers,

All my post-graduate mates, and all department of Mechanical Engineering,

Tebessa University teachers,

Acknowledgment

I thank Allah who gives me the patience to finish this work

My parent for their support

My supervisor Dr. Abdallah Diha for the useful

comments, remarks and encouragements and teaching us new things through the learning process of this master work

And I would like to thank the jury for their acceptance to examine

this work

And sincere thanks to each of the characters help to finish this work.

.

Contents

Chapter one: bibliographical study

Chapter Three: Results and discussions

List of Figures

List of Tables

List of Symbols

Symbol	Meaning	Unit
W	The mass	G
I	The current	A
E	The chemical equivalent weight	G
T	The time	S
F	constant called the Faraday	-
m	Mass Molar	G
M	Molar mass	Mol
C	The concentration	mol/l
V	The volume	L
A	The expansion coefficients	K^{-1}
P	The pressure	Bar
$\mathbf{d_{hkl}}$	Inter-planner Spacing	Å
hkl	the miller indices	-
Θ	Diffraction Angle	Degree
$\mathbf{a}^{\mathbf{2}}$	Atomic distance	Nm
$\mathbf{D_{hkl}}$	The average grain size	-
$\boldsymbol{\beta_{hkl}}$	The full width at half maximum intensity	-
$\mathbf{T_C}$	Texture Coefficient	-
N	Reflection number	-
E	The strain	-
$\mathbf{a_o}$	Lattice Constant	Å
Δ	Dislocation Density	cm^{-2}
$\mathbf{D_{av}}$	The Crystallite Size	Nm
T	The thickness	Nm
$\mathbf{N_0}$	The number of crystallites	cm^{-2}
$\mathbf{I_o}$	Incident intensity	mW/cm^2
$\mathbf{I_A}$	Absorbed light intensity	mW/cm^2
T	Transmittance	-
A	Absorbance	-
$\mathbf{E_g}$	Energy Band gap	Ev
$\mathbf{E_u}$	Urbach energy	MeV
Λ	Wavelength of Incident Light	Nm
$\boldsymbol{h\nu}$	Photon Energy	eV
$\mathbf{R_s}$	Sheet resistance	Ω/square
$\mathbf{R_b}$	The bulk resistivity	Ω/Cm
$\mathbf{\Delta_m}$	The weight difference	G
$\mathbf{A_S}$	Area	Cm^2
$\boldsymbol{\rho_0}$	The Density of Material	g/cm^3

List of Abbreviations

Symbol	Meaning
TCO	Transparent Conductive Oxides
MO	Metal oxide
TBL	Thermal Barrier Layer
Ni	Nickel
NiO	Nickel Oxide
Cu	Copper
CNO	Copper nickel oxide
F.C.C	Face-Centered Cubic
EUV	Evaporation Under Vacuum
CS	Cathode Sputtering
PLD	Pulsed Laser Deposition
TE	Thermal Evaporation
CBD	Chemical Bath Deposition
CVD	Chemical Vapor Deposition
SPT	Spray Pyrolysis Technique
XRD	X-Rays Diffraction
UVS	UV-visible Spectrophotometer
ASTM	American Standard for Testing of Materials
JCPDS	Joint Committee for Powder Diffraction Standards

General introduction

General Introduction :

Today, modern products offer even more new functions with the unusual properties that often cannot be found in bulk sample. These product materials open completely new areas of applications. The multi functionality of these technical products especially concerns their surface properties. Surface coating of glass with different types of films is one of the technologies that occupy a key position in the material and product development. Transparent Conducting Oxide (TCO) thin films are deposited on transparent substrates to form transparent electrodes. Transparent electrodes is the key component of a variety cutting-edge applications, such as solar cells, gas sensors, organic light-emitting diodes, liquid crystal displays, electro chromic smart windows, as well as architectural coatings [1].

Deposition of high quality, uniform thin films, is an intensive area of research which has yielded many varied deposition techniques each technique falls into one of three broad categories: wet chemical deposition; physical vapor deposition and chemical vapor deposition. Careful selection of the appropriate deposition technique is essential for control over the properties of the resultant films. Different techniques can affect growth rates, crystalline [2].

Nickel oxide (NiO) exhibits wide features in it's the optical, magnetic and electrical properties behavior related to electronic structure. Which forms the basis for the enormous range of applications such as supercapacitor, electrochromic device, photo-catalytic; it is an anti-ferromagnetic semiconductor oxide. It can be prepared in the form of conducting thin films by various techniques that involve: electron beam evaporation, magnetron sputtering, chemical deposition, sol–gel and spray pyrolysis technique (SPT).

In our present work, will be chose the spray pyrolysis method to prepare thin films of nickel oxide on glass samples because it is simple and low cost. Then will be studied some of the structural, optical and electrical properties of these films.

In this work, thin layers of Copper doped nickel oxide (NiO: Cu) prepared with different percentage of the doped copper (0, 0.5, 1.5, 3, 6 %) are produced using a solution Nickel Nitrate and Copper Chloride as a precursor to prepare good quality and homogeneity thin films on glass substrates by chemical spray pyrolysis technique (SPT) at temperature of (420 ±20 °C). The work was carried out at the Laboratory of Materials Engineer at the University of Tebessa.

The main objective of this work is study the effect of Cooper doping Nickel Oxide on : structural, optical and electrical characteristics using different characterization techniques such as : X-ray diffraction for micro-structural characterization, UV-visible spectroscopy for optical characterization, four-point technique for electrical measurements and weight difference method for thickness measurement.

This work consists of three chapters organized as follows:

It was starting with a general introduction.

In the first chapter, we will provide a bibliographic study starting by define the thin film.This study was followed by presenting its crystallographic, optical, electrical and chemical properties. The nickel oxide was used related of its remarkable properties and its multitude applications. Then this study was completed by presenting some propriety of Copper. At the end, we will provide description of Solar cells and photodetectors and Photocatalysis.

The second chapter contained two parts which have consisted respectively detailed explanation of the different deposition techniques and we are focused on the spray pyrolysis method used in the present work for our thin layers and the second part include the characterization techniques such as UV spectrometer and X-ray defraction .

The third chapter contains the experimental methods used in preparing and getting the doped and undoped thin films and we will explain and analyze the obtained results and finally give a general conclusion on it.

Chapter one: bibliographical study

I.1 Introduction:

Nowadays, most of the technologies are used for minimizing the materials into nano-size as well as nano-thickness leading to the emergence of new and unique behaviors of such materials in optical, electrical, dielectric applications, and so on. Hence, a new branch of materials science is called thin films or coatings that we will talk about it in this chapter.

I.2 Definition of thin films:

A thin film is a layer of material ranging from fractions of a nanometer to several micrometers in thickness. Electronic semiconductor devices and optical coatings are the main applications benefiting from thin-film construction. A familiar application of thin films is the household mirror, which typically has a thin metal coating on the back of a sheet of glass to form a reflective interface. The process of silvering was once commonly used to produce mirrors. A very-thin-film coating is used to produce two-way mirrors. The performances of optical coatings are typically enhanced when the thin-film coating consists of multiple layers having varying thicknesses and refractive indices. Similarly, a periodic structure of alternating thin films of different materials may collectively form a so-called superlattice which exploits the phenomenon of quantum confinement by restricting electronic phenomena to two-dimensions. Work is being done with ferromagnetic and ferroelectric thin films for use as computer memory. It is also being applied to pharmaceuticals, via thin-film drug delivery. Thin-films are used to produce thin-film batteries. Thin films are also used in dye-sensitized solar cells [3].

Thin film also can be defined as a thin layer of material, where the thickness is varied from several nanometers to few micrometers. Like all materials, the structure of thin films is divided into amorphous and polycrystalline structure depending on the preparation conditions as well as the material nature. Thin films comprise two parts: the layer and the substrate where the films are deposited on it. Also, thin films can be composed of different layers such as thin-film solar cells, electrochromic cells, and so on [4].

I.2.1 Principle of deposit of thin films:

To form a thin layer on a solid surface (substrate) the particles of the coating material must pass through a conductive medium until intimate contact with the substrate. When the substrate arrives, a fraction of the coating particle adheres or reacts chemically with the substrate. The particles can be atoms, molecules, ions or fragments of ionized molecules. The transport medium can be solid, liquid, gas, or vacuum:

a) **Solid:** in this situation, the substrate is in contact with the solid, only the particles which diffuse from the solid towards the substrate form a layer. Often, it is very difficult to obtain thin films by contact between solids, for example: the diffusion of Oxygen from Silica to form a thin SiO_2 layer on a Silicon substrate.

b) Liquid medium: it is easier to use than the first case, because the material is more versatile in this state (epitaxial in liquid phase, and electrochemical, sol gel…).

c) Gas or vacuum: this is a CVD type deposit where the difference between the gaseous medium and the vacuum is the average free path of the particles. There is no standard thin film deposition method that can be used in different situations. Substrate preparation is often a very important step for thin layer deposits in order to obtain good adhesion [5].

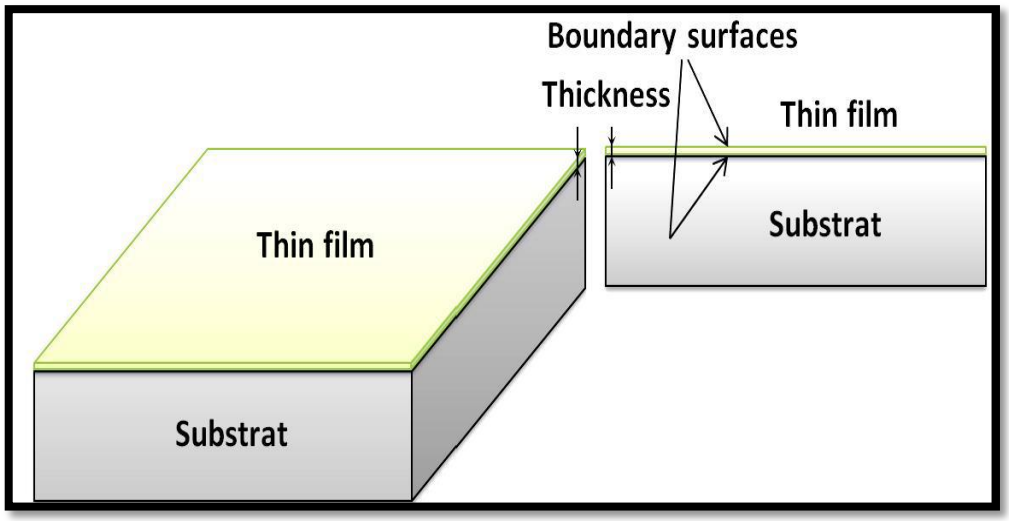

Figure I.1: Schematic of thin film deposited on a glass substrate [5].

I.2.2 Formation of thin films:

The deposition process of a film can be divided into three basic phases:

1. Preparation of the film forming particles (atoms, molecules, cluster)
2. Transport of the particles from the source to the substrate
3. Adsorption of the particles on the substrate and film growth

These phases can depending on the specific deposition process and/or on the choice of the deposition parameters is considered as either independent or as influencing one another. The former is desirable since it allows controlling the basic steps independently and therefore yields a high flexibility in the deposition process [6].

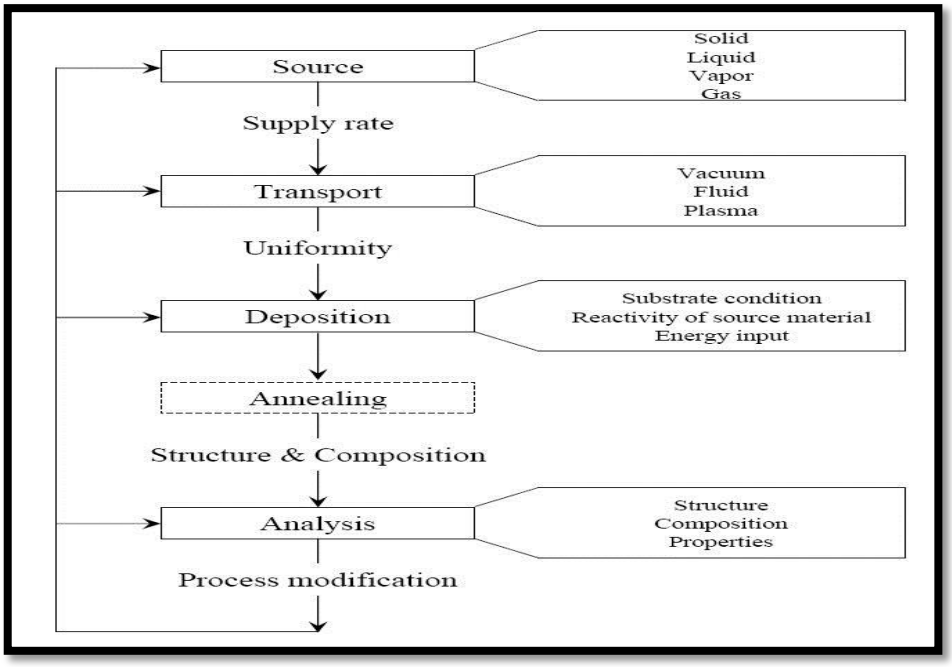

Figure I.2: the steps of the thin film manufacturing process [7].

I.2.3 Interest and characteristics of thin films:

The interest of thin layers comes mainly from the economical use of materials in relation to the physical properties and the simplicity of the technologies used for their realization. A wide variety of materials are used to produce these thin layers. By putting them, we cite metals, alloys, refractory compounds (Oxides, Nitrides, and Carbides), intermetallic compounds and polymers.

The essential characteristic of a thin layer, whatever the procedure used for its manufacture, is that it is always integral with a support on which it is built (even if it sometimes happens that we separate the thin film of said support) . Consequently, it will be imperative to take this major fact into account in the design, namely that the support very strongly influences the structural properties of the layer which is deposited there.

Thus, a thin layer of the same material, of the same thickness, may have substantially different physical properties depending on whether it is deposited on an amorphous insulating substrate such as glass or a monocrystalline Silicon substrate for example. It follows from these two essential characteristics of a thin layer the following consequence A thin layer is anisotropic by construction. In practice, we can distinguish two main families of thin layer production methods, those which use a carrier gas to move the material to be deposited from a container to the substrate and which are similar to the diffusion techniques used in the manufacture of active components, and those which

involve an environment at very reduced pressure and in which the material to be deposited will be conveyed thanks to an initial pulse of thermal or mechanical nature [8].

I.2.4 Thin film growth mechanism:

Thin film is prepared by deposition of the film materials (metals, semiconductors, insulators, dielectric, etc.) on a substrate through a phase transformation. Sufficient time interval between the two successive deposition of atoms or molecules and also layers are required so that these can occupy the minimum potential energy configuration. In thermodynamically stable films, all atoms (or molecules) will take up positions and orientations energetically compatible with the neighboring atoms of the substrate or to the previously deposited layers, and then the effect substrate or the initial layers will diminish gradually [9].

The deposition process of a film can be divided into three basic phases:

1. Preparation of the film forming particles (atoms, molecules, cluster);
2. Transport of the particles from the source to the substrate;
3. Adsorption of the particles on the substrate and film growth.

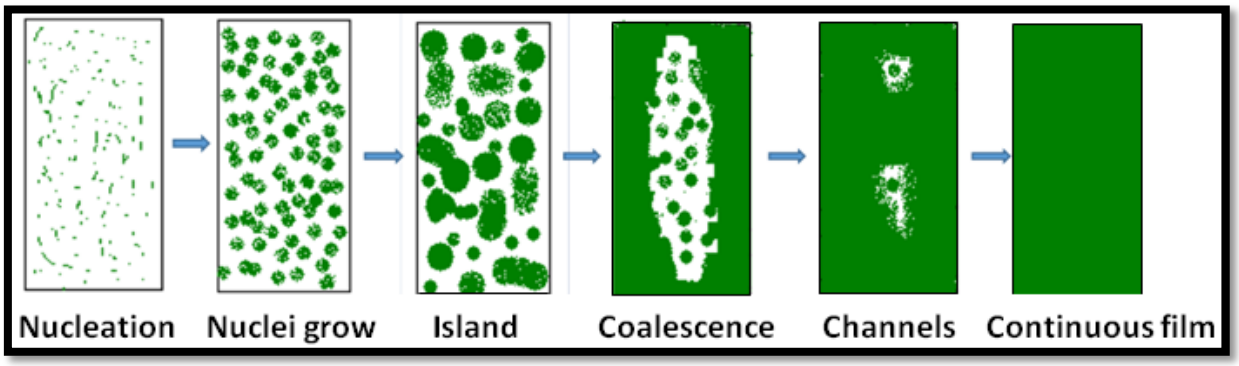

Figure I. 3: Various stages of nucleation and growth of thin films [7].

For more understanding thin films, the following properties illustrate various mechanisms occurring at different stages of film growth. There are several stages in the growth process, from the initial nucleation of the deposits to the final continuous three dimensional film formation states:

I.2.4.1. Nucleation:

The nucleation is the primary process for all deposition. The common process of addition, adsorption, desorption, migrations, etc. of atoms is called nucleation or small cluster formation which is schematically shown in (figure I-3-a) [10].

I.2.4.2. Island structure:

The islands consist of comparatively larger nuclei (>10 Å) and generally of three dimensional natures with their height, however, much less than their lateral dimensions. The formation of these islands and their growth take place either by direct addition of atoms from the vapor phase or from other environment or by the diffusion controlled process (see figure I-3-b). The diffusion controlled process is moreover commonly observed except at low substrate temperature.

I.2.4.3. Coalescence:

As mentioned in the second stage, as islands grow they develop some characteristic shapes and then with further growth, coalesce with the neighboring ones by rounding off their edges near the joining region (neck) where these deposits assume a liquid like structure. The coalescence involves considerable transfer of mass between islands by diffusion. Small islands disappear rapidly. The process resembles the sintering of bulk powder where the individual particles assume spherical shapes due to the lowering of their surface energies. During coalescence of two islands which occurs at their necks recrystallization as well as annealing takes place leading to some definite shapes of larger islands (figure I-3-c and d).

I. 2.4.4 Channel and Holes:

As the coalescence continues with deposition, there will be a resultant network of the film with channels in between (figure I-3-e). These channels do not remain void, but the secondary nuclei start to grow within these void spaces in the channel. Sometimes these channels may not be completely filled up even with increasing film thickness thus leaving some holes or gaps in the aggregate mass (see figure I-3-f). With increasing film thickness, these holes or gaps will decrease in size.

I.2.4.5. Continuous film:

When these gaps are completely bridged by the secondary nuclei, films will be continuous. However, it often happens that some void space may still remain unabridged. In an ideal continuous film there should not be any gap in the aggregate mass. Such a stage in the film can be attained at certain average film thickness (figure I-3-g) [11].

I.2.5 Applications of thin films:

Engineering/Processing

- biological Applications: Protective coatings to reduce wear, corrosion and erosion, low friction coatings
- Hard coatings for cutting tools
- Surface passivation
- Protection against high temperature corrosion
- Self-supporting coatings of refractory metals for rocket nozzles, crucibles, pipes
- Decorative coatings
- Catalyzing coatings

Optics

- Ant reflex coatings ("Multicoated Optics")
- Highly reflecting coatings (laser mirrors)
- Interference filters
- Beam splitter and thin film polarizers
- Integrated optiques

Optoelectronics

- Photo detectors
- Image transmission
- Optical memories
- LCD/TFT

Electronics

- Passive thin film elements (Resistors, Condensers, Interconnects)
- Active thin film elements (Transistors, Diodes)
- Integrierted Circuits (VLSI, Very Large Scale Integrated Circuit)
- CCD (Charge Couple Devise)

Cry technics

- Superconducting thin films, switches, memories
- SQUIDS (Superconducting Quantum Interference Devises)

New Materials

- Super hard carbon ("Diamond")
- Amorphous silicon
- Metastable phases: Metallic glasses

- Ultrafine powders (diameter < 10nm)
- Periodization of high melting point materials (diameter 1-500μm)
- High purity semiconductors (GaAs)

(Alternative) Energies

- Solar collectors and solar cells
- Thermal management of architectural glasses and foils
- Thermal insulation (metal coated foils)

Magnetic Applications

- Audio, video and computer memories
- Magnetic read/write heads

Sensors

- Data acquisition in aggressive environments and media
- Telemetry
- Biological Sensors

Biomedicine

- Biocompatible implant coatings
- Neurological sensors
- Claddings for depot Pharmacia [6].

I.3 Fundamental properties of Nickel (Ni), Nickel Oxide (NiO), and Copper (Cu) material:

I.3.1 Nickel (Ni):

Nickel is a chemical element with the symbol Ni and atomic number 28. It is a silvery-white lustrous metal with a slight golden tinge. Nickel belongs to the transition metals and is hard and ductile [12].

I.3.1.1 Physical and Chemical Properties:

- Atomic Symbol: Ni
- Atomic Number: 28
- Element Category: Transition metal
- Density: 8.908 g/cm3
- Melting Point: 1455 °C
- Boiling Point: 2913 °C

- Moh's Hardness: 4.0 [12].

I.3.1.2 Characteristics:

- Nickel is a hard, silvery-white metal, which is malleable and ductile.
- The metal can take on a high polish and it resists tarnishing in air.
- Nickel is ferromagnetic and is a fair conductor of heat and electricity [12].

I.3.1.3 Application:

- The majority of nickel is used in corrosion-resistant alloys, such as stainless steel.
- Many coins contain nickel.
- Nickel steel is used for burglar-proof vaults and armor plate.
- Nickel is also used in batteries – for example NiCd (nickel-cadmium) and Ni-MH (nickel-metal hydride) rechargeable batteries – and in magnets [12].

I.3.2 Nickel oxide (NiO):

Nickel oxide is the chemical compound with the formula NiO. It is the principal oxide of nickel. It is classified as a basic metal oxide.

I.3.2.1 Physical and Chemical Properties:

- Average atomic number: 18
- Average atomic mass (g): 27.35
- Molar mass (g / mol): 74.69
- Boiling point (° C) > 2000
- Solubility in water (mg / L): 1.1 at 20 ° C. insoluble
- Melting point (° C): 1990 – 1960
- Enthalpy of formation at: 298k -240 KJ / mole of atoms
- Entropy S0 (KJ.mol-1): 38.0

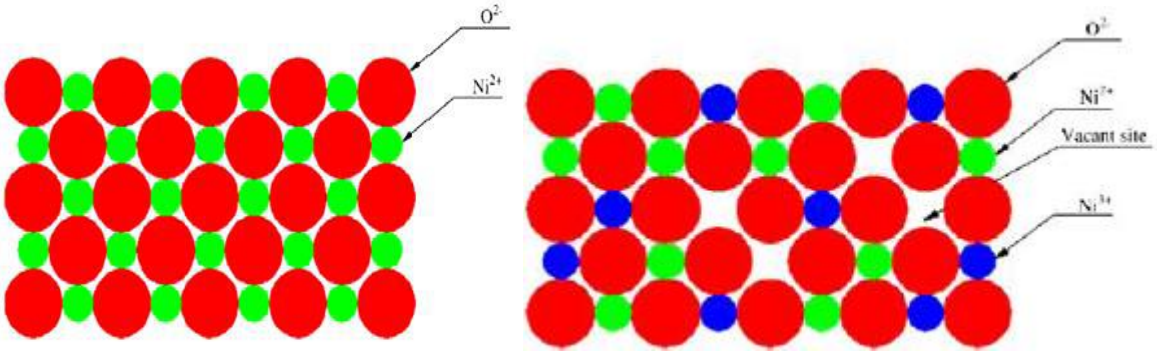

Figure I.4: Structure of nickel oxide [10].

I.3.2.2 Crystallographic and structural properties:

Nickel oxide (NiO) crystallizes in a NaCl structure (rock salts)**.** It has a face-centered cubic structure-type (FCC). This cubic structure is composed of two similar sub networks A and B, so that every atom of subnet A has only neighbors belonging to subnet B and vice versa. The anionic sub network (O^{2-}) and the cationic sub network (Ni^{2+}) have a CFC structure. The plane (100) is a mixed plane composed of 50% nickel and 50% oxygen. The planes (111) are alternately pure Ni and pure O. The face (111) is a polar face (non-stable) against the face (100) is a non-polar face (stable).

Crystalline solids show a periodic in its crystal structure. Perfect stoichiometric metal oxides are insulators but by introducing different defects inside the crystal, its electrical, optical and mechanical properties changes. It should be noted that the existence of the defects depends on the growth method and the material development conditions [13].

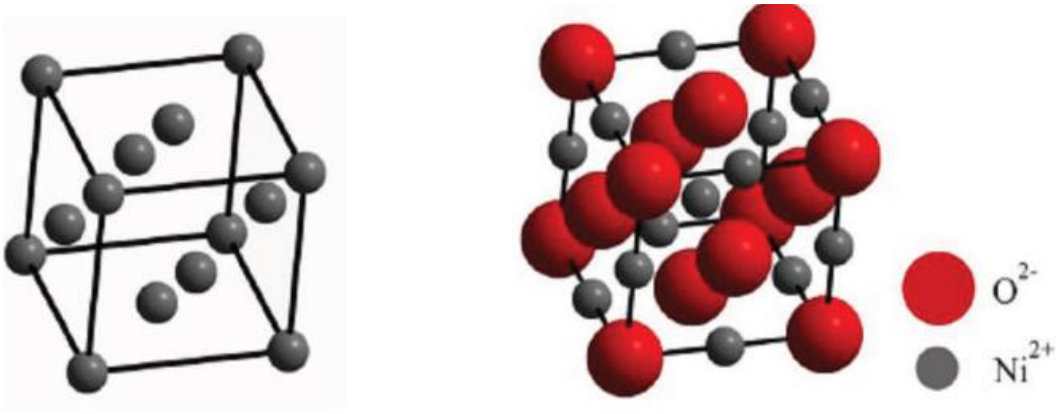

Figure I.5: Crystallographic structure of nickel oxide [13].

I.3.2.3 Electrical properties:

Nickel oxide NiO has p-type oxide semiconductor character with broadband gap energy. Nominally pure stoichiometric NiO is an insulator as in Figure I.4 with a room temperature resistivity of the order of 10^{13} Ω-cm is classified as a Mott-Hubbard insulator. Various theories have been done to explicate the insulating behavior of NiO; they include localized electron theory, band theory, chemical band approach and cluster theory. After intense theoretical and experimental investigations, the electronic structure of NiO remains controversial [14].

Table I.1: Some electrical properties of NiO [13].

Properties	Values
Conductivity type	P
Electrical conductivity ($(\Omega.cm)^{-1}$)	10^{-6}-10^{-1}
Hall coefficient (cm^3/C)	5-120
Charge carrier density (cm^{-3})	10^{17}-10^{18}
Mobility (cm^2/ V.s)	0.1- 7.6

I.3.2.4 Optical properties of NiO:

Nickel oxide is a transparent material in the visible with a wide optical gap of 3.6 to 4 Ev. The transmittance is varied between 40% - 80% and the refractive index is of the order of 2.18. Preparation conditions, deposition methods, and doping are the parameters that influence the optical properties of NiO [15].

Nickel oxide have high conductivity and lighting gap energy directly, NiO is green due to strong absorption in violet (2.75 – 2.95 eV) and red 1.75 eV. In case of excess oxygen, namely Ni is oxidized by directly oxygen or doping with Li+, high absorption coefficient of the green range (1.75 – 2.75 eV) is expanded and NiO appears as black.

Band gap of NiO thin films changes with the deposition technique in between 3.6 and 4 eV. To understand the electronic structure of NiO, various optical experiments have been carried out such as photoemission or inverse photoemission studies. Theoretical calculations about optical spectra have also been reported. There are some significant points about conduction band, valence band and optical band gap of NiO to be noticed:

1. Ni 3d states dominate the conspicuous structure at valence band edge.

2. Ni 4s is located at the conspicuous structure of conduction band edge, but the structure on the small shoulder (Ec-E) ~ 0.8 eV) is detected and considered as localized Ni states.

3. The gap of band structure is clean due to its nature; however, mid-gap structure is quite sensitive susceptible to thin film deposition and defects [11].

I.3.2.5 Different Applications of Nickel Oxide Thin Films:

Recently, NiO thin films were increased rapidly due to their importance in many applications in science and technology. NiO is one of the important P-type classes of

semiconducting materials, which has attracted a good amount of research interest. This is because of the fact that NiO has unique optical, electrical and magnetic properties and founds a vast diversity of applications in energy efficient smart windows, automobile mirrors, building glazing, optoelectronic devices and hetero-junction solar cells… etc. Nickel oxides is a wide band gap, low cost, advantageous ion storage material in points of cyclic stability and find applications in electrochromic devices transition metals, which reversibly changes the optical properties in the presence of electric field. Furthermore, NiO was applied to produce the Ni-Cd rechargeable batteries. NiO is now exploited in the recyclable protein separation and as biosensors. In addition, there are many applications and properties of nickel oxide based materials were investigated and proved in the field of antimicrobial activity, control infections and excessive antibiotic resistance [16].

I.3.3 Some properties of cooper:

Copper is non-polymorphous metal with face centered cubic lattice (FCC, Fig. 6). Pure copper is a reddish color; zinc addition produces a yellow color, and nickel addition produces a silver color. Melting temperature is 1083 °C and density is 8900 $kg.m^{-3}$, which is three times heavier than aluminum. The heat and electric conductivity of copper is lower compared to the silver, but it is 1.5 times larger compared to the aluminum [17].

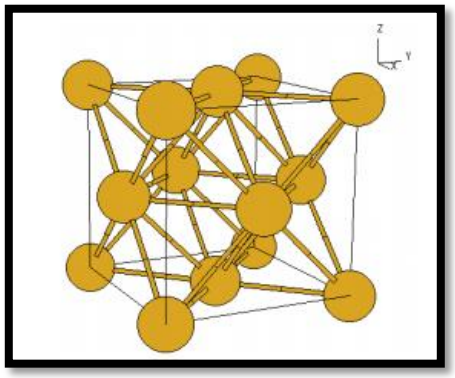

Figure I.6: FCC lattice [17].

I.4 Solar cells and photodetectors:

In general metal oxides (MO) are mostly non-toxic with obvious chemical stabilization and important abundance in nature, also manufactured using inexpensive methods under ambient conditions. MO-based devices are inexpensive, very stable, and environmentally safe. 10 years ago, it was difficult to use these materials as semiconductors but nowadays a lot of companies sell products based on these materials [18]. Thus, MO-based semiconductors are promising for third generation solar cells.

I.4.1 Solar cells:

Metal oxides materials play an integral part of the photovoltaic industry as they serve as the transparent electrode for solar cells such as amorphous silicon solar cells, dye-sensitized solar cells and organic based photovoltaic devices. MO materials are most useful in that they are simply fabricated on a large scale via online processes. There are certain requirements however when choosing a MO to serve as the electrode for a photovoltaic device. Matching photovoltaic performance to the MO is vital and it should be well-known that:

- as the MO layer thickness increases the current of short circuit decreases;
- the charge carrier density of the MO decreases the current of the short circuit in the PV device;
- The band gap matching of the MO with the solar spectrum can result in high exchange efficiencies.

In addition to the requirements mentioned above the MO layer must have high durability, high adhesion and show resilience to high processing temperatures often required for thin film solar cell manufacturing [19].

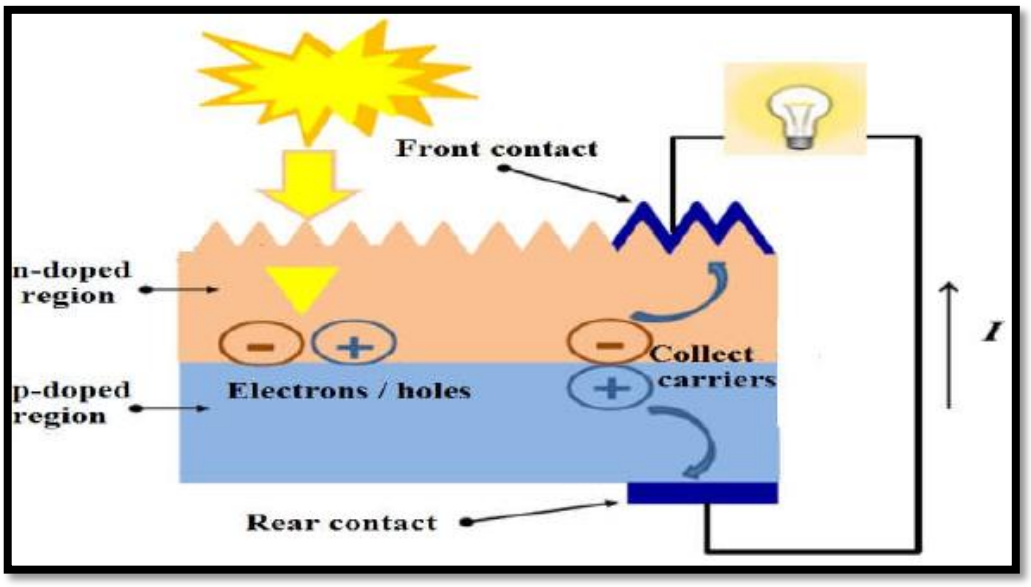

Figure I.7: illustrates the operating principle of a conventional photovoltaic cell called the first generation [19].

When photons of incident light with energies greater than or equal to the band gap of the semiconductor material are absorbed by the p-n junction, electron/hole pairs are created.

Electrons are excited from the valence band into the conduction band leaving holes at valence band and by collecting those charges the electric energy will produce.

Cu_2O /NiO is an example of a heterojunction solar cell, where the Cu_2O is spontaneously p type and NiO is n-type as shown in figure I.8. This junction is working well because the conduction band edges of Cu_2O and NiO align well. Cu_2O is a good absorption layer material, and NiO nanowires allow for good charge transport, high band gap and large interface, the latter allowing for thicker films and thus higher absorption [14].

Crystallographic orientation is important for achieving a good photoresponse for a p- Cu_2O /n-NiO cell [16]. However, the efficiency is still very low.

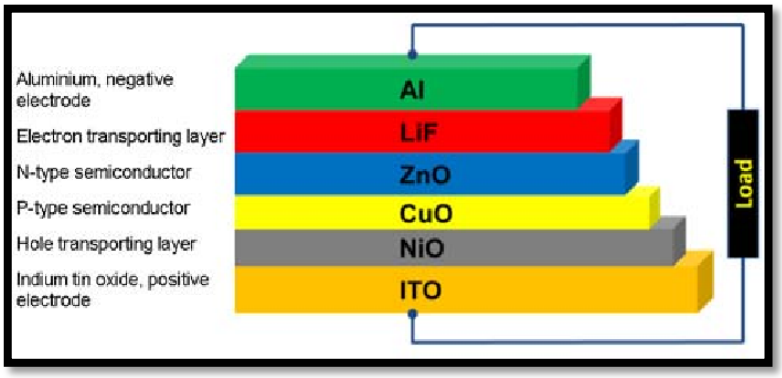

Figure I. 8: Representation of Cu_2O /NiO heterojunction solar cell [7].

I.4.2 Photodetectors:

Photodetectors are used in a variety of applications in many fields like compact disc players, optical-fiber communications, and surveillance of rockets or intercontinental ballistic missiles, remote sensing…. They are basically semiconductor devices that can detect an optical signal and convert it into an electrical signal. The operation of a general photodetector basically operates as a solar cell. Figure I.9 summarized the operating mechanism on three processes: first, carrier generation by incident light then second, carrier transport and/or multiplication then third, extraction of carriers as terminal current to provide the output signal [20].

Three main types of photodetectors are generally used: photoconductors, photodiodes, and phototransistors.

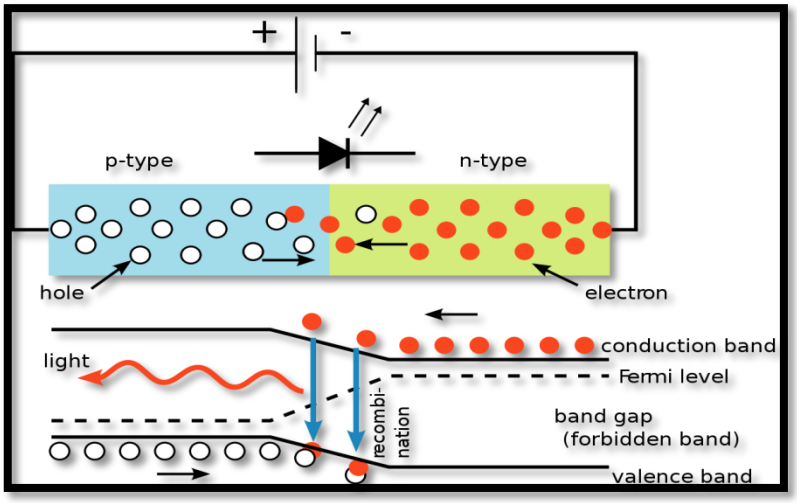

Figure I. 9: Operating Mechanism of the photodiode p-n junction [7].

I.5 Photocatalysis:

Photocatalysis is the procedure that enables change of solar energy into chemical energy needed for the decomposition of dyes or organic pollutants. The photocatalytic reactions usually occur on the semiconductor's surface. Metal oxide semiconductor (MOS) are considered as activators that help in catalyzing the complex radical chain reaction involved in the photocatalytic oxidation processes [21]. Generally, metal oxide photocatalysis is achieved using developed oxidation method which is realized by exercising a strong oxidizing species of OH radicals usually produced in situ. The OH radicals form the trigger to initiate a sequence of reactions that crumbles the complex dye macro-molecule into simpler and smaller, less harmful components [22].

I.5.1 The basic principle of photocatalysis:

A photocatalytic reaction is initiated while the particle of material semiconductor absorbs photon energy, this energy more than its gap energy. The photo-excited electron is moved from valence band energy (VB) to the conduction band energy (CB). The electron-hole pairs were created and diffused out to the surface of the photocatalyst and participate in the chemical reaction with the electron donor and acceptor groups of a compound. The electron-hole pairs modify the adjoining oxygen or water molecules into OH free radicals with super strong oxidization leading to stable end products as shown in Figure I.10 [23].

.

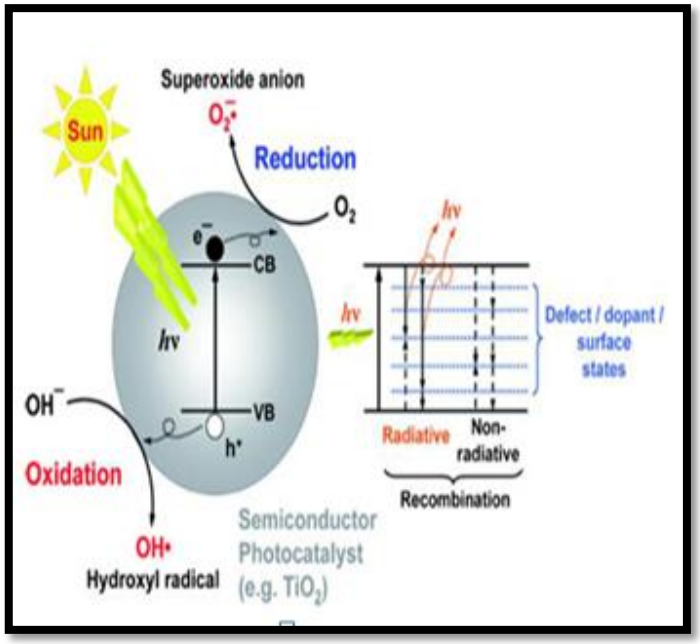

Figure I.10: Schematic diagram explaining the principle of photocatalysis [21].

I.6 Semiconductor photocatalysis:

Since Fujishima and Honda reported in 1972 the water splitting into H_2 and O_2 using titanium dioxide (TiO_2) electrode, semiconductor-based photocatalysis has garnered considerable attention because of its application potential in wastewater treatment and the production of hydrogen fuel using solar or ultraviolet light. P-type semiconductors are rarely used in photocatalytic semiconductors and generally, only n-type semiconducting oxides are used. NiO, CdS, Fe_2O_3, tungsten oxide (WO_3) are the best known of semiconductor photocatalysis but their photocatalytic activity is lower than that of titanium dioxide (TiO_2) which is the most useful photocatalyst for the environmental application.

Photocatalyst semiconductors are essentially wide bandgap semiconductors. Therefore, the photons must have high energies to generate electrons from the valence band to the conduction band. In general, these photons belong to the UV part [24]. There are many approaches to obtain semiconductor with a photocatalytic activity under solar radiation and different photocatalytic systems were used. We intend to use the systems shown in figure I.11 (b).

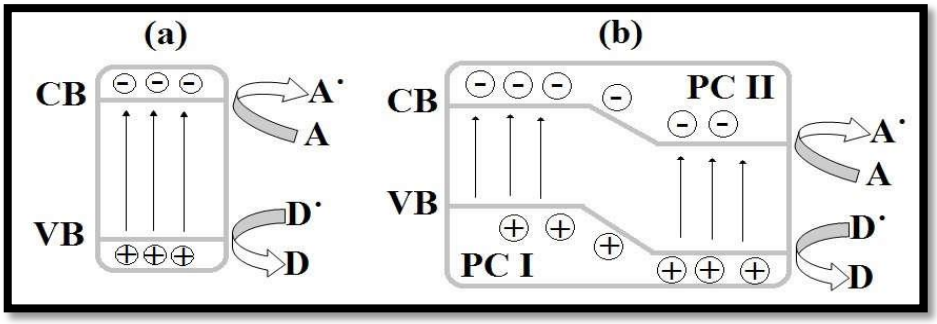

Figure I. 11: Schematic diagrams of photocatalyst systems we used a) Single photocatalyst, (b) type II heterojunction. (PC I: photocatalyst I, PC II: photocatalyst II) [24].

In general, studies focus on the development of efficient photocatalytic materials and attempt to obtain the following characteristics:

- High-efficiency photocatalysts which absorb a large amount of solar energy (ability to generate electron-hole pairs)
- High charge separation (electron-hole pairs).
- Less expensive and easier to produce, non-toxic and durable.

Mainly the position of the edge of the semiconductor band is one of the most important and useful parameters to be considered for use as a photocatalyst**.** Figure I.12 shows the positions of the band edge of several commonly used semiconductors. It should be noted a certain important parameter such as; the position of VB must be lower than the oxidation potential of oxygen and CB must be greater than that of hydrogen, also the importance of the presence of grain boundaries and surface states on the semiconductor to allow the electrons/ holes pairs generated to reach the pollutant species [25].

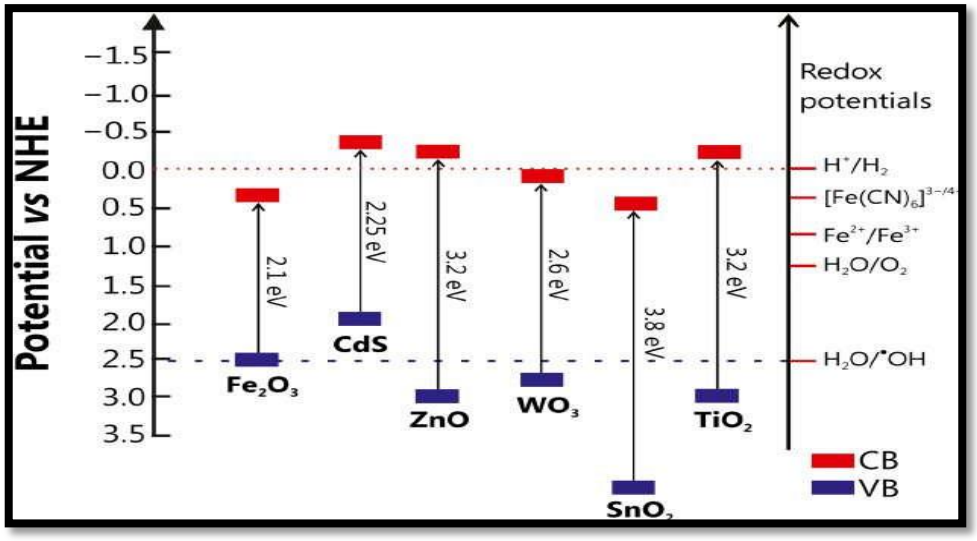

Figure I.12: Band positions of commonly used semiconductors with respect to the redox potentials of oxidizing species [25].

In order to design an efficient photocatalyst, heterojunction systems are one of the approaches offering good charge separation, reduced charge recombination, and increased optical absorbance range, allowing for better photocatalyst performance. Photocatalysis of nanoscale semiconductors also provides a considerable amount of sites per volume/mass that promotes the reactions [26].

I.7 Conclusion:

In this chapter we have known the definition of thin films and we give a bibliographic overview of nickel oxide (NiO) and cooper by introducing their structural, optical and electrical properties. Also we present a general outline of the potential applications of metal oxides including solar cells, photodetectors and the photocatalysis application.

Chapter two:

Methods of deposition and characterization techniques

II.1 Introduction:

The deposition ways of the thin layers are different from one another. It refers to the diversity of the domain where we use these layers. Scientifically, these ways are divided into two parts: physical and chemical such as Spray pyrolysis which is the spot of our study in this work.

II.2 Thin film Deposition Technique:

The properties of thin films are extremely sensitive to the method of preparation, several techniques have been developed (Depending on the desired film properties) for the deposition of the thin films of the metals, alloys, ceramic, polymer and superconductors on a variety of the substrate materials. Each methods has its own merits & demerits and of course no one technique can deposit the thin films covering all the desired aspects such as cost of equipment's, deposition conditions & nature of the substrate material etc [27].

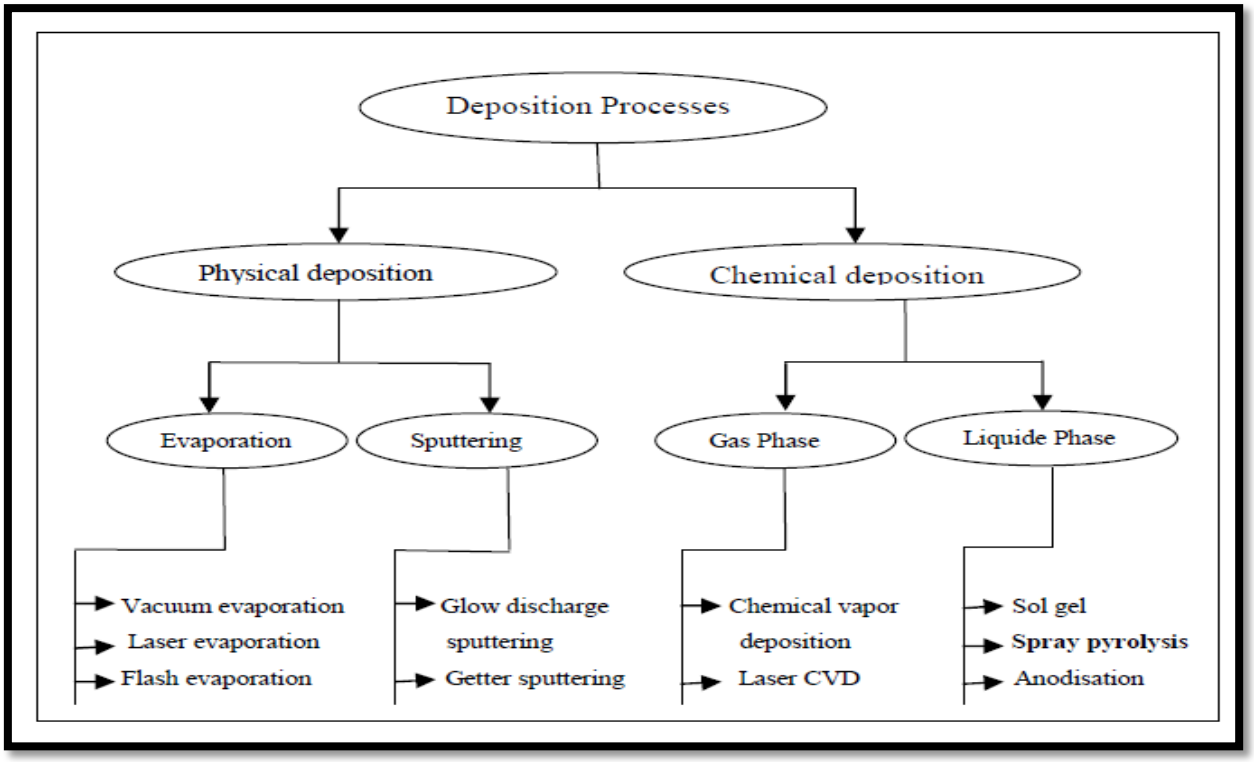

Figure II.1: Classification of thin Film deposition techniques [27].

II.2.1. Physical techniques:

Physical method covers the deposition techniques which depend on the evaporation or ejection of the material from a source, i.e. evaporation or sputtering [28].

II.2.1.1. Evaporation:

Evaporation is a physical vapor deposition (PVD) process in which the wafer (substrate) is placed in a chamber and subjected to very low pressures as the chamber are removed using a vacuum pump. One the chamber is free of residual gases, the material to be deposited is subjected to a temperature sufficient to cause it to evaporate. The evaporated molecules are dispersed throughout the chamber, landing on the wafer (and the chamber walls) and condensing, coating the wafer uniformly. Evaporation or sublimation techniques are widely used for the preparation of thin layers. A very large number of materials can be evaporated and, if the evaporation is undertaken in vacuum system, the evaporation temperature will be very considerably reduced; the amount of impurities in the growing layer will be minimized [29].

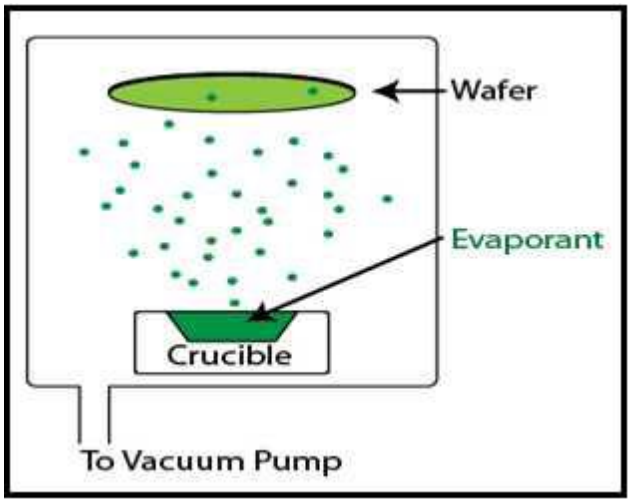

Figure II.2: Schematic diagram of the evaporation technique [30].

II.2.1.2. Sputtering:

Sputtering is another physical vapor deposition process occurs in a vacuum chamber. A large piece of the material to deposited, known as a target, is bombarded with high energy argon ions from a glow discharge. When the argon ions strike the target, they knock off target atoms and molecules, which are then conveyed through the vacuum to the wafer (i.e. substrate), where they condense and form a thin film. Sputtering is most commonly used for depositing metal films, but, like evaporation, can also deposit insulating films with some slight process and equipment variations [31].

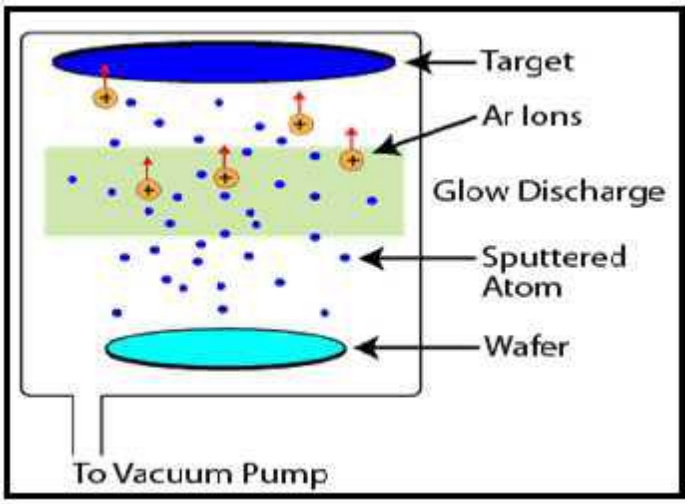

Figure II.3: Schematic diagram of the sputtering technique [33].

Each method has his advantages and disadvantages as it recapitulated in table II.1**.**

Table II.1: Advantages and Disadvantages of Physical process [34].

Deposition Process	Advantages	Disadvantages
Evaporation	- Highest purity - To low pressures.	- Lower throughput due to low vacuum. - High cost.
Sputtering	- Better step coverage. - Less radiation damage than evaporation.	- Some plasma damage including implanted argon - High cost.

II.2.2. Chemical Process:

Chemical methods depend on physical properties. Structure-property relationships are the key features of such devices and basis of thin film technologies. Underlying the performance and economics of thin film components are the manufacturing techniques on a specific chemical reaction [35].

II.2.2.1. Chemical Vapor Deposition:

Chemical vapor deposition can be defined as a material synthesis method in which the constituents of vapor phase react together to form a solid film at surface. The chemical reaction is an essential characteristic of this method; therefore, besides the control of the

usual deposition process variables, the reactions of the reactants must be well understood. Various types of chemical reactions are used in CVD for the formation of solids are pyrolysis, reduction, oxidation, hydrolysis, synthetic chemical transport reaction etc., a numbers of forms of CVD in wide use and are frequently referenced in the literature [36].

a) Metal-organic CVD (MOCVD), CVD processes based on metal-organic precursors;

b) Photo-Enhanced Chemical Vapor Deposition (PECVD);

c) Laser-Induced Chemical Vapor Deposition (LCVD);

d) Low-pressure CVD (LPCVD), CVD processes at sub atmospheric pressures. Reduced pressures tend to reduce unwanted gas phase reactions and improve film uniformity across the wafer;

e) Plasma-enhanced CVD (PECVD), CVD processes that used plasma to enhance chemical reaction rates of the precursors. PECVD processing allows deposition at lower temperatures, which is often critical in the manufacture of semiconductors.

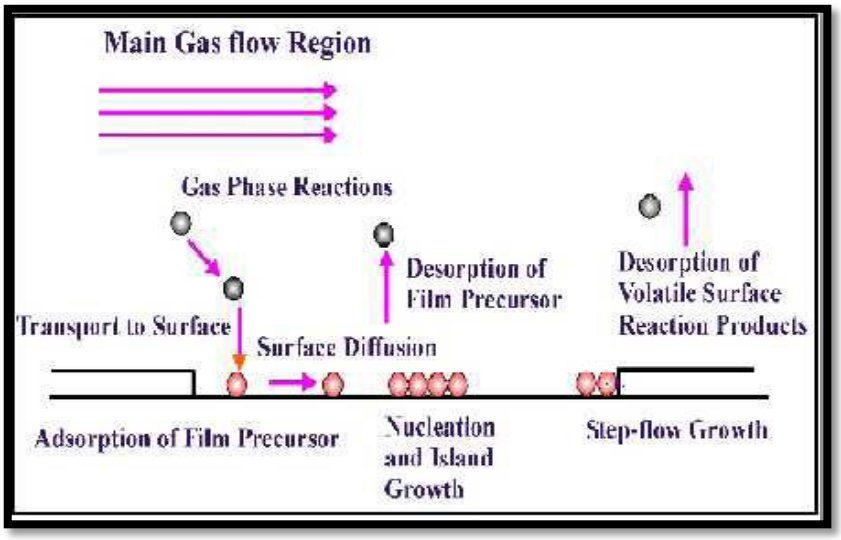

Figure II.4: Deferent stages of chemical vapor deposition (CVD) process [37].

II.2.2.2. Sol-gel:

Sol-Gel is a chemical method using for preparation of metal oxide-type materials such as ceramics and glasses. Initially, it consists of a stable suspension (Sol) of chemical precursors in solution. These "Sol" was transformed to a "Gel" during the gelling step result of chemical interactions between species in suspension and solvent, to give an expanded three-dimensional solid lattice through the liquid medium. The obtained gel is "wet" subsequently it was transformed into dry amorphous material by removal of solvents

(to obtain an air-gel) or by evaporation under atmospheric pressure (to obtain xerogel) [38].

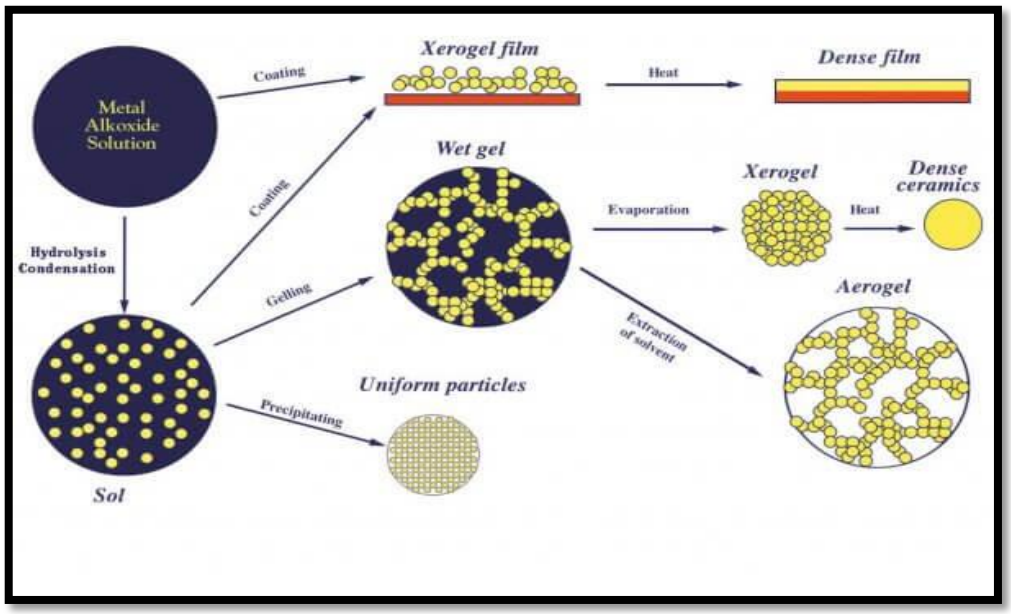

Figure II.5: Sol-gel mechanism [7].

Each method has his advantages and disadvantages as it recapitulated in table II.2**.**

Table II.2: Advantages and disadvantages of chemical process [38].

Deposition Process	Advantages	Disadvantages
Chemical Vapor Deposition	- The versatility of the CVD process. - Materials in excess 99.9% of theoretical density. - Economical in production, since many parts can be coated at the same time.	- CVD tends to increase the cost of fabrication. - Limitation can be overcome using single source chemical precursors. - The use of more sophisticated reactor and/or vacuum system by CVD variants.
Sol gel	- Smaller particle size and morphological control in powder synthesis. - Sintering at low temperature also possible. - provides high purity homogeneous materials	- High cost of the precursors. - Long process duration. - Difficulties in the synthesis of monoliths.

In all deposition process, atoms collect on the substrate in structures that initially have low density and low order compared to the equilibrium structure of the film material. The mechanisms by which crystallographic order is gradually recreated within the deposited film have been subjects of intense study.

II.2.3 Spray Pyrolysis:

Different processes for the preparation of films have been employed, such as: physical vapor deposition (PVD), chemical vapor depositions (CVD), sol-gel and spray pyrolysis. However, Compared to the other techniques mentioned, spray pyrolysis requires simple and inexpensive equipment and has as main advantages the easy addition of doping materials, good reproducibility, high films growth rate, chemical homogeneity in the final product and the potential for deposition over large areas. The films, dense or porous, have thicknesses ranging from 0.1 to 10 μm [39].

Spray pyrolysis is a technique through which dense or porous films and powders can be obtained by controlling the deposition parameters. This technique involves the atomization of a precursor solution that is thrown directly over the heated substrate where the film will be formed [40].

II.2.3.1. Principle:

Spray pyrolysis involves a thermally stimulated chemical reaction between constituent ions to form the required compound. In this technique, a solution containing the soluble salts of the constituent atoms of the required compound is sprayed on to a hot substrate in the form of fine droplets, using a sprayer. Usually compressed air will be the carrier gas. But compressed nitrogen is also used as carrier gas to avoid the presence of oxygen. The sprayed droplets reaching the hot substrate surface undergo pyrolytic decomposition and form the compound as a thin film on the surface of the hot substrate. In fact it is the hot substrate which provides the thermal energy needed for the decomposition and subsequent recombination of the constituent species. The other volatile by products and the excess solvents are converted into vapor phase and are removed from the site of chemical reaction by using an exhaust fan [41].

The following atomizers are usually used in spray pyrolysis technique:

- Air blast (the liquid is exposed to a stream of air).
- Ultrasonic (ultrasonic frequencies produce the short wavelengths necessary for fine atomization).
- Electrostatic (the liquid is exposed to a high electric field) [42].

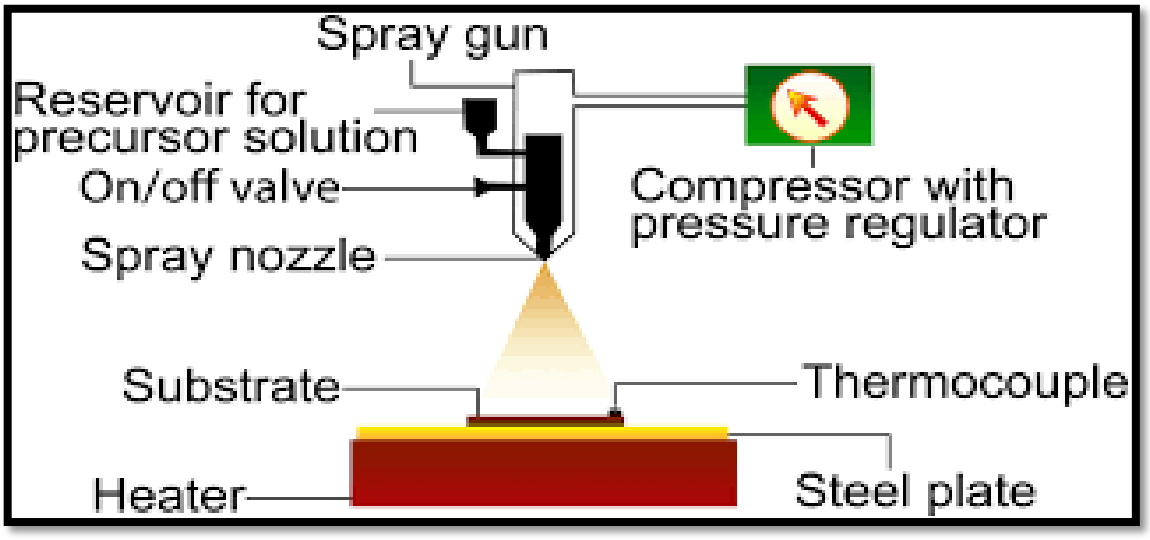

Figure II.6: The schematic of the spray pyrolysis [7].

II.2.3.2. Processing steps of spray pyrolysis technique:

Spray pyrolysis involves many processes occurring either simultaneously or sequentially. The most important of these steps are three processing steps that are presented and analyzed as follows:

1. Atomization of the precursor solution;

2. Aerosol transport of the droplet;

3. Decomposition of the precursor to initiate film growth [43].

a) Precursor atomization:

The atomization procedure is the first step in the spray pyrolysis deposition system. The idea is to generate droplets from a spray solution and send them, with some initial velocity, towards the substrate surface. Spray pyrolysis normally uses air blast, ultrasonic, or electrostatic techniques [44].

b) Aerosol transport of droplets:

After the droplet leaves the atomizer, it travels through the ambient with an initial velocity determined by the atomizer. In the aerosol form, the droplets are transported with the aim of as many droplets as possible reaching the surface. As the droplets move through the ambient, they experience physical and chemical changes depicted in figure I1.7 [45].

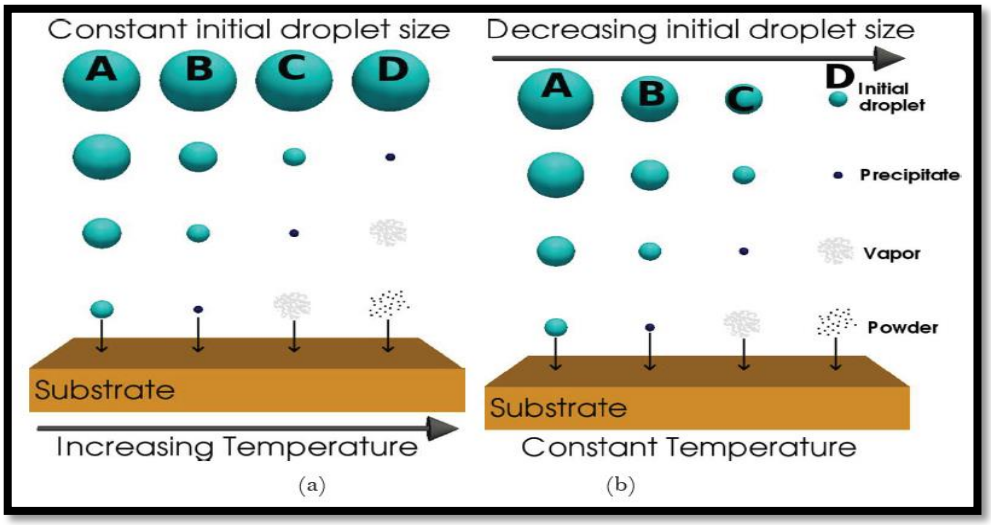

Figure I1.7: Diagram of the different process stages for the aerosol droplet evolution as it approaches the hot substrate for two cases: (a) Constant initial droplet size and increasing substrate temperature, and (b) constant substrate temperature and decreasing initial droplet size [45].

c) Precursor decomposition:

The precursor, as it moves through the heated ambient undergoes various changes. Evaporation, precipitate formation, and vaporization all occur depending on the droplet size and ambient temperature. The droplet may interact with the substrate surface. Although all processes occur during deposition, process C, the CVD like deposition is desired to yield a dense high quality film [46].

When the processing environment causes droplets to evaporate prior to reaching the substrate vicinity, a precipitate will form early. As the precipitate reaches the immediate vicinity of the substrate, it is converted into a vapor state and it undergoes a heterogeneous reaction through the following steps:

1) Reactant molecules diffuse to the surface.

2) Adsorption of some molecules at the surface.

3) Surface diffusion and a chemical reaction, incorporating the reactant into the lattice.

4) Desorption and diffusion of the product molecules from the surface.

This is a classical CVD reaction, which results in a high quality film deposition and a high sticking probability.

4) Process D: high temperature - small droplet size: When small initial droplets are formed, or the temperature is high enough, the droplet quickly forms a precipitate. As the precipitate approaches the substrate, it is vaporized and a chemical reaction subsequently

occurs in the vapor phase. This homogeneous reaction leads to the condensation of molecules into crystallites in the form of a powder precipitate. The powder falls to the substrate surface, but without a deposition reaction [47].

II.2.3.3 Influence of the some main spray pyrolysis technique (SPT) parameters on the quality of the deposited films:

This section deals with the influence of the some main SPT parameters on properties of the deposited films.

a) Influence of the temperature:

The deposition temperature is involved in all mentioned processes, except in the aerosol generation. Consequently, the substrate surface temperature is the main parameter that determines the shape and properties of the film [48]. By increasing the temperature, the film morphology can change from a cracked to a porous microstructure.

In many studies the deposition temperature was reported indeed as the most important spray pyrolysis parameter. The properties of deposited films can be varied and thus controlled by changing the deposition temperature; it influences structural, optical and electrical properties of thin films [49].

b) Influence of precursor solution:

The precursor solution is the second important process variable. The solvent, salt type, salt concentration and additives affect the physical and chemical properties of the precursor solution. Thus, many properties of the deposited film can be changed by changing the composition of the precursor solution. Such as film thickness, morphology, chemical structure, and electrical and optical properties [50].

c) Influence of atomizer (nozzle)-to-substrate distance:

This parameter has the similar effects resembling the atomizing air pressure. In fact both these parameters are mutually dependent. The decreasing nozzle-substrate distance will introduce the nozzle tip to the increasingly hot ambient which can result into the blockage of the nozzle. Conversely increasing nozzle-substrate distance will increase the aerosol traverse path. This will cause the aerosols to experience thermal energy further and either powdered films or no deposition will result. Therefore, it is suggested that the nozzle-substrate distance and atomizing air pressure should be optimized mutually [51].

II.2.3.4 Advantages of chemical spray pyrolysis technique:

In our work chemical spray pyrolysis technique has been chosen for preparation of NiO nanostructured layers because it has a number of advantages:

1. Spray pyrolysis is a simple and low cost technique for the preparation of semiconductor thin films.
2. It has capability to produce large area, high quality adherent films of uniform thickness.
3. Spray pyrolysis technique does not require high quality targets or substrates nor does it require vacuum at any stage, which is a great advantage if the technique is to be scaled up for industrial applications.
4. The deposition rate and the thickness of the films can be easily controlled over a wide range by changing the spray parameters.
5. A major advantage of this method is operating at moderate temperature (200–6000C) and can produce films on less robust materials.
6. Not like high-powered strategies like frequency electron tube sputtering (RFMS), it doesn't cause native heating that may be prejudicial for materials to be deposited. There are nearly no restrictions on substrate material, dimension or its surface profile.
7. By dynamic composition of the spray solution throughout the spray method, it is often used to create bedded films and films having composition gradients throughout the thickness.
8. It's believed that reliable elementary kinetic information are additional seemingly to be obtained on significantly well characterized film surfaces, provided the films area unit quiet compact, uniform which no aspect effects from the substrate occur. SPT offers such a chance [52].

II.3 Thin film Characterization Techniques:

The growth mechanism and properties of the films can be well understood by their characterizations using a variety of investigative techniques. Before using the films in applications, one has to characterize the films to achieve optimum performance of the films prepared. The complete characterization of any material consists of compositional characterization, structural elucidation, micro-structural analysis and surface characterization, which have strong bearing on the properties of materials. In order to perform this in a systematic way, one needs a diverse array of characterization techniques.

To confirm this, in this element we will describe the various characterization techniques utilized in our work:

1. Weight difference method.
2. X-Ray diffraction technique (XRD): for the study of structural properties.
3. Ultra-violet-visible spectroscopy (UV-Vis) for the study of optical properties.
4. Method of four probes for the study of electrical properties [53].

II.3.1. Weight difference method:

The most common and important factor is the film thickness in the investigation of the sample properties. Different techniques were used for estimating the film thickness, the weight difference method is simple and convenient and thickness t is measured using the gravimetric method.

II.3.1.1 The gravimetric method:

This method is done by using sensitive electronic balance with four digits sensitivity (10^4g). The substrates are weighted before and after deposition. From the weight difference and the area of substrate, the thin film thickness (t) can be measured, according to the following equation:

$$\mathbf{T = \Delta m / \rho_0 \times A_S} \qquad \text{(II.1)}$$

Where:

Δm = is the weight difference of substrate. This means that it is the mass of the thin film (g). A_S= area of the thin film Cm^2,

ρ_0: the density of material of the thin film (6.67 g/ Cm^3) for nickel oxide and (8.96 g/cm^3) for cooper, the density of material calculated from:

*Total density (ρ_0) = density of NiO × its percentage in the solution + density of Cu × its percentage in the solution [54].

II.3.2. X-Ray diffraction Techniques:

X-Ray diffraction technique (XRD) is one of the most useful characterization methods as it can provide a great deal of information about the film without requiring much sample preparation.

Much of our knowledge about crystal structure and the structure of molecules as complex as DNA in crystalline form comes from the use of x-rays in x-ray diffraction studies. A basic instrument for such study is the Bragg spectrometer [55].

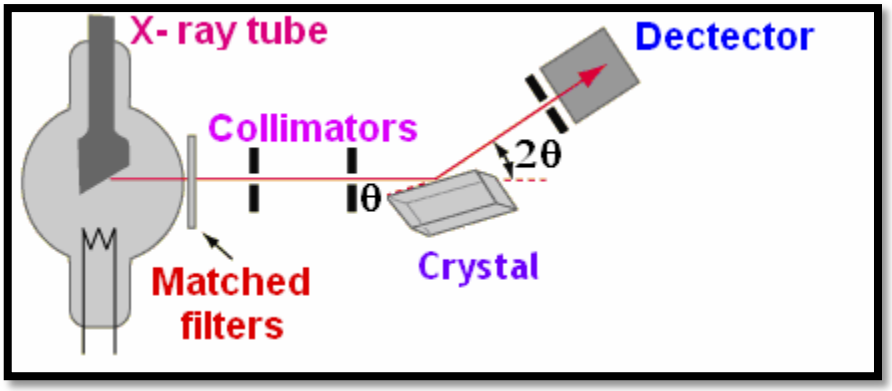

Figure II.8 (a): Bragg Spectrometer [55].

Figure II.8 (a): and Figure II.8 (b): shows the schematics of X-ray diffractometer. Diffraction in general occurs only when the wavelength of the wave motion is of the same order of magnitude as the repeat distance between scattering centers. This condition of diffraction is nothing but Bragg's law and is given as:

$$2d_{hkl}\sin\theta_{hkl} = n\lambda \qquad \text{(II.2)}$$

Where,

d_{hkl} = interplaner spacing the spacing between the parallel planes in the atomic lattice,

(*h, k and l*) = are the miller indices of the corresponding lattice planes (*hkl*),

θ_{hkl} = diffraction angle is the angel between the incident ray and the scattering planes,

λ = wavelength of x-ray beam,

n = order of diffraction (an integer =1),

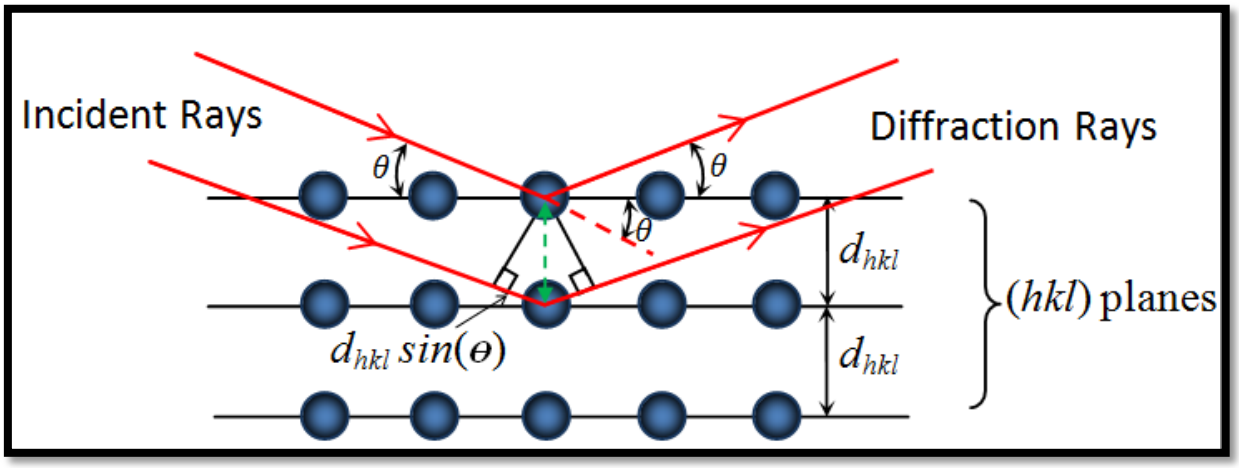

Figure 1I.8 (b): Schematic of X-ray diffraction According to Bragg [56].

X-ray diffraction studies give a whole range of information about the crystal structure, orientation and average crystalline size of the films. The diffraction patterns obtained experimentally of the sample are compared with the standard patterns of the likely elements and compounds present in the sample. Based on this comparison conclusions can be drawn about crystal structure and orientation of the sample.

II.3.2.1 Information obtained from the X-ray diffractogram:

There is much information that we can deduce from the X-ray diffractogram, some of which are presented below.

a) grain size:

From the X-ray diffraction pattern, the width generated in a peak which known as full width at half maximum (FWHM) (See figure II.8), can be used to calculate the mean crystallites sizes of the film in a direction perpendicular to the respective (*hkl*) planes, by using the Scherrers formula [57] which is given as:

$$D_{hkl} = \frac{0.9\lambda}{\beta_{hkl}\cos(\theta_{hkl})} \qquad \text{(II.3)}$$

Where:

D_{hkl}: is the average grain size obtaining from the peak (hk1).

λ: is the wavelength applied for X-ray of (λ= 1.5406 Å).

β_{hkl}: is the full width at half maximum intensity of the peak (hk1).

θ_{hkl}: is the angel between the incident ray and the (hk1) scattering planes.

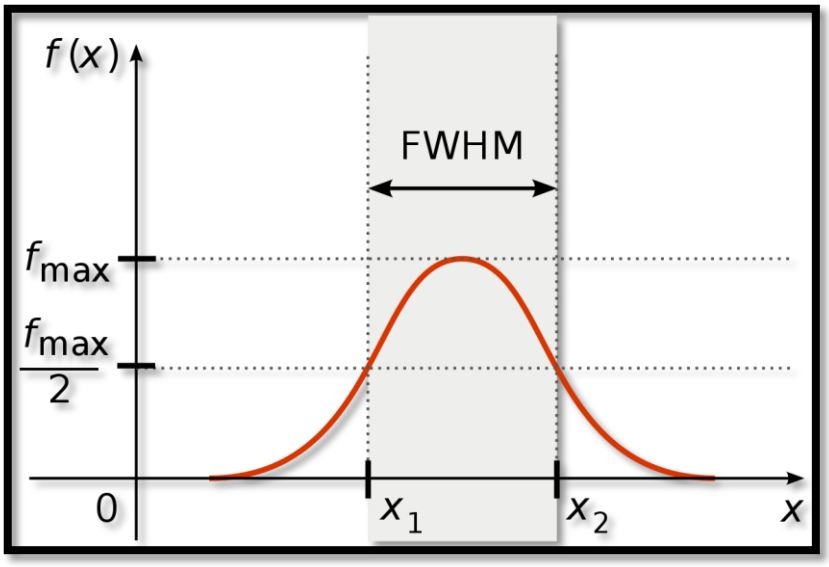

Figure II.9: Full width at half maximum (FWHM) of an arbitrary peak [55].

b) Lattice parameters:

Using *d* values, the series of lattice planes (*h k 1*) were identified from standard data. Strong peaks are expected when the condition of Bragg is satisfied. The lattice parameter values for different for the cubic systems can be determined from the following equation [58]:

$$d_{hkl} = \frac{a_{hkl}}{\sqrt{h^2 + k^2 + l^2}} \qquad \text{(II.4)}$$

c) The texture coefficient:

The texture coefficient Tc illustrates the texture (the distribution of crystallographic orientations of a polycrystalline sample) of the specific plane, deviation of which from unity reveals the preferred growth. About the preferential orientation quantitative information was effectuated from the different texture coefficient Tc (hkl) defined as [59]:

$$T_c(hkl) = \frac{I(hkl)/I_0(hkl)}{\frac{1}{N}\sum_N I(hkl)/I_0(hkl)} \qquad \text{(II.5)}$$

Where:

I (hk1): is the relative experimental intensity from (hkl) plane, I_0 (hk1)is the intensity of standard pattern from the JCPDS information and N is the reflection number.

II.3.3. Spectroscopy UV- visible:

Spectrophotometers are optical devices that determine the light intensity of reflected or transmitted using objects with a variation of wavelength. Light throughout the lamp enters the monochromator, which makes the light dispersion and selects the particular wavelength chosen by the operator for the measurement. After that, the chosen wavelength is moved alternately throughout the sample and along the reference path. The reference and sample light beams pass via the cell compartment, consisting of a reference space and a sample space. The two light beams converge on the detector. Transmittance or absorbance of solid or liquid and total diffuse reflectance/transmittance of solids like large disks, silicon wafers, plastics, glass etc. can be measured. Band gap determination, electron transition and enzyme activity studies can also be made [60].

A diagram of the typical constituent of the spectrophotometer is represented from the Figure II.10. By using diffraction grating or prism the beam of light (visible or/and UV light source) is divided, into its component wavelengths. By a half-mirrored device, every monochromatic beam is dividing into two equal intensity beams. One beam, the sample beam (colored magenta), proceed through a small transparent container (cuvette) comprise a transparent solvent or solid like thin films being studied. The further beam, the reference (colored blue), carry on through the same cuvette including just the solvent. The intensities of these beams of light are then examined using electronic detectors and comparator.

The beam intensity (reference beam) defined as I_0, which becomes small or no light absorption. However the beam intensity of the sample defined as I. Over a short period of time, automatically the spectrometer sweeps all the component wavelengths from the previous description. The ultraviolet (*UV*) portion is studied from 200 to 400 nm, and the visible section is ranged in 400-800 nm. If the sample does not absorb light of a given wavelength, $I=I_0$. Furthermore, if the sample absorbs light then I is less than I_0, and this variation may be plotted on a graph versus wavelength. Absorption was displayed as transmittance ($T = I/I_0$) or absorbance ($A= \log I_0/I$). If no existence of absorption so $T = 1.0$ and $A= 0$ [61].

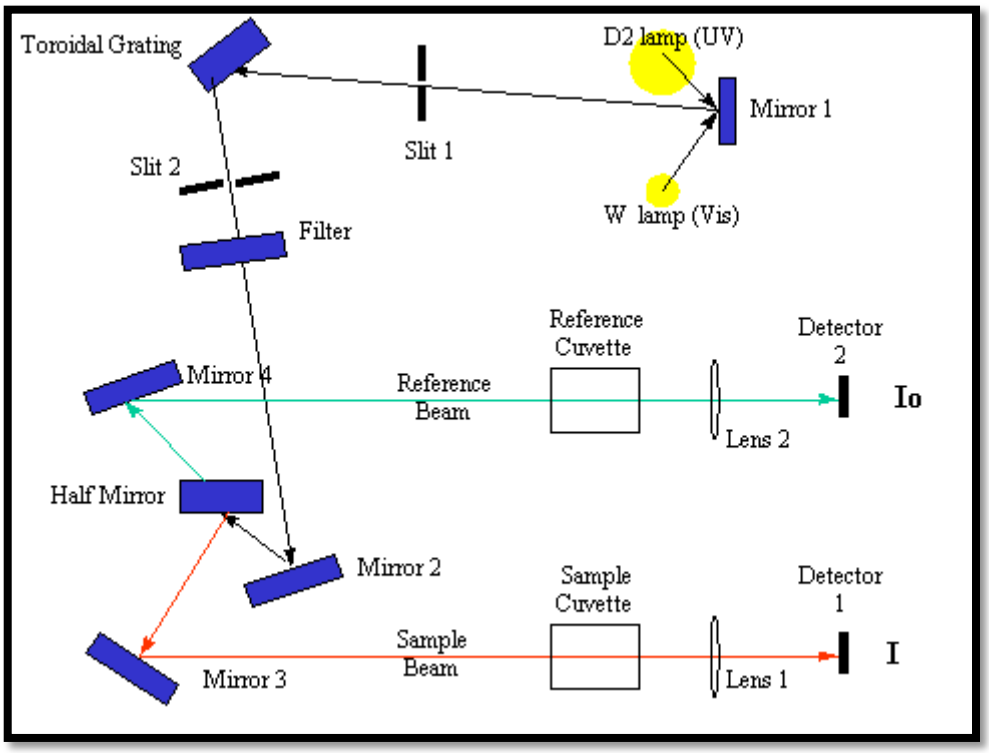

Figure II.10: Schematic representation of UV-Visible spectrometer [61].

II.3.3.1 Information obtained from the UV-visible transmittance spectra:

Using UV-Vis spectroscopic data we can calculate: absorption coefficient, band gap energy and Urbach energy.

a) Absorption coefficient:

The absorption coefficient α of hematite film was determined from transmittance measurements. The films absorption coefficient was calculated using the following expression [62]:

$$T = e^{-\alpha d} \tag{II.6}$$

$$\alpha = -\frac{1}{d}\ln(T) \tag{II.7}$$

Where: T is the normalized transmittance,

d: is the film thickness,

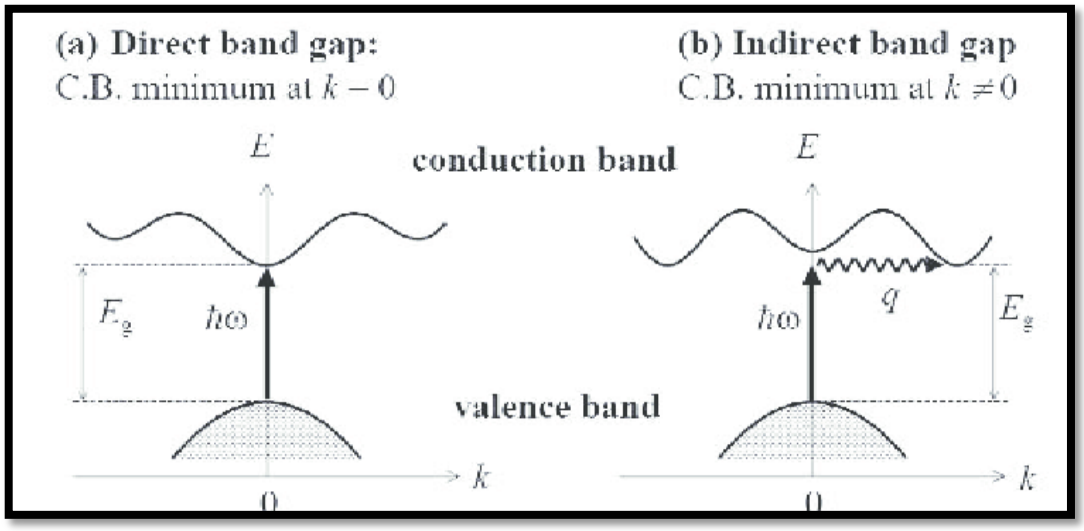

Figure II.11: diagram showing (a) direct band and (b) indirect band transition [7].

b) Optical band gap energy:

The optical gap energy is one of the fundamental characteristics of optical materials. The measurement of gap energy relies not only on the material but also on its characteristics and stoichiometry. The energy limited to the highest maximum of the band of valence the and lowest minimum of the band of conduction is known as band gap energy (E_g). By determination of the absorption coefficient values, E_g value can be evaluated by the Tauc's formula [61]:

$$(\alpha h\nu)^2 = B\,(h\nu - E_g) \qquad \text{(II.8)}$$

Where:

B: is a constant which does not correlate to the photon energy,

α : is the absorption coefficient,

(hν): is the photon energy and.

Direct band gap was evaluated using extrapolating the straight-line portion $(\alpha h\nu)^2$ as a function of (hν) to the energy axis at zero absorption coefficient (α=0) as observed from figure II.12.

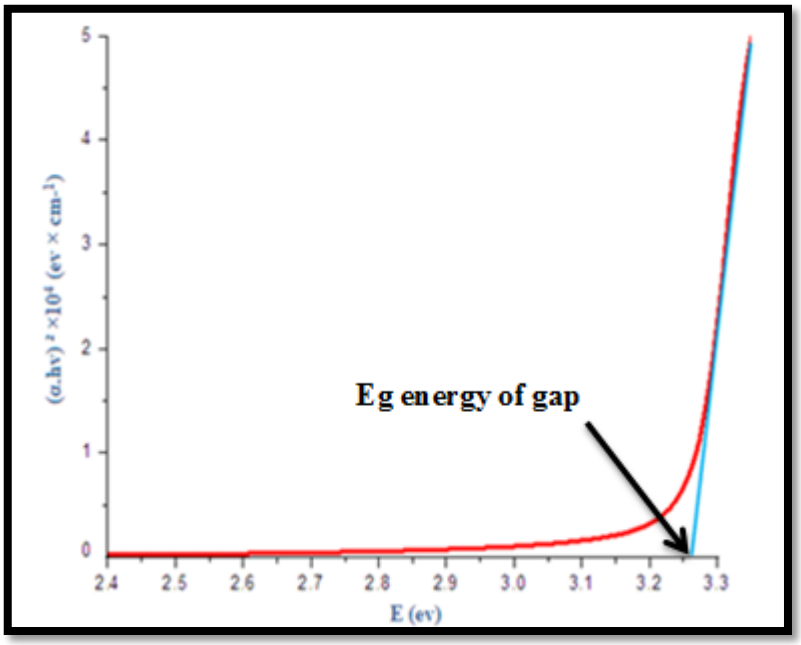

Figure II.12: Determination of the energy gap E*g* by the extrapolation method from the variation of $(\alpha h\nu)^2$ as a function of $h\nu$ for a thin layer [7].

c) Urbach Energy:

Urbach energy defined as the width of the localized states available in the optical band gap that affects the optical band gap structure and optical transitions. The Urbach tail is determined by the following relation (Urbach 1953) [63]:

$$\alpha = \alpha_0 \exp(\frac{h\nu}{E_u}) \qquad \text{(II.9)}$$

Where :

α_0 : Constant;

hv : The photon energy

E_u: Urbach energy, which refers to the width of the exponential. It is possible to determine the value of urbach energy E_u through drawing a statement ln α as function of hv:

$$ln\ \alpha = ln\ \alpha_0 + (h\nu/Eu) \qquad \text{(II.10)}$$

Therefore, the band tail energy or Urbach energy (Eu) can be obtained from the slope of the straight line of plotting ln(α) against the incident photon energy (hv).

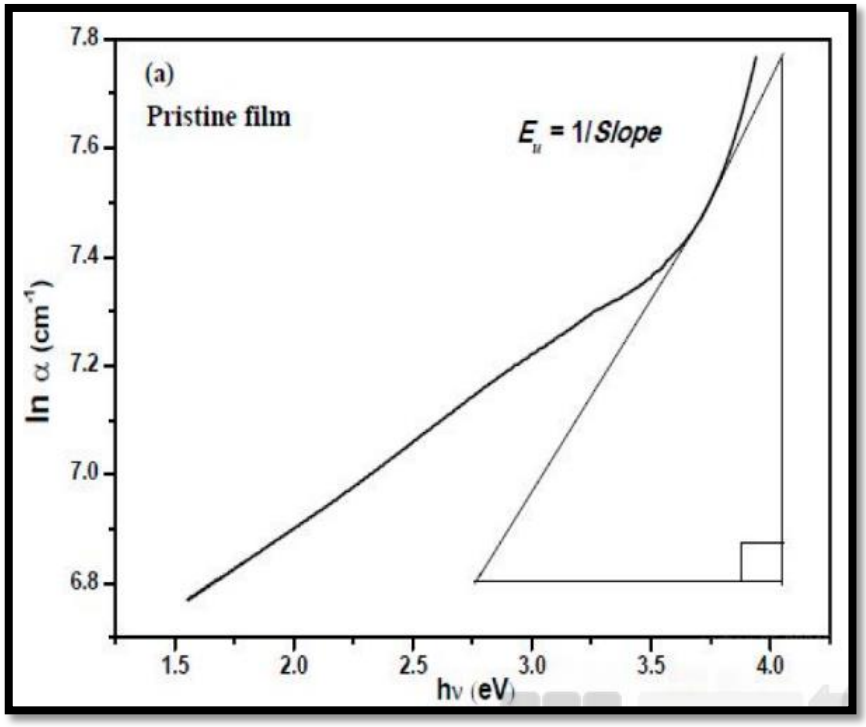

Figure II.13: determination of the Urbach energy from the variation of ln(α) as a function of *hv* for a thin layer [63].

II.3.4 The four-point method:

The 4-point probe set up figure (II.14) consists of four equally spaced tungsten metal tips with finite radius. Each tip is supported by springs on the end to minimize sample damage during probing. The four metal tips are part of an auto-mechanical stage which travels up and down during measurements. A high impedance current source is used to supply current through the outer tow probes; a voltmeter measures the voltage across the inner two probes, to determine the sample resistivity. Typical probe spacing is ~ 1 mm [64]:

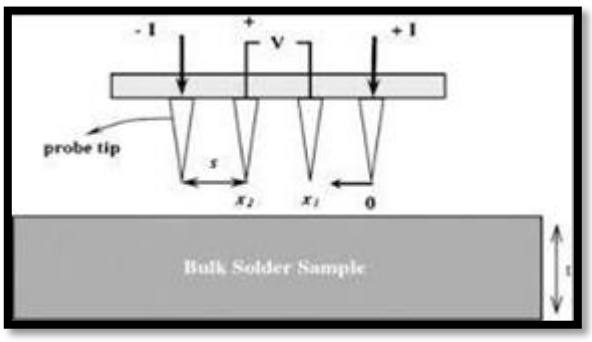

Figure II.14: Schematic of four point probe configuration [64].

In figure II.14 for the Four probe method, s is spacing between point probes, it unit by meter (m).

The two outer probes are used for sourcing current and the two inner probes are used for measuring the resulting voltage drop across the surface of the sample. The volume resistivity is calculated as follows [65]:

$$\rho = \frac{\pi}{\ln 2} \cdot \frac{V}{I} \cdot d \qquad \text{(II.11)}$$

Where:

ρ : The volume resistivity ($\Omega \cdot cm$);

V: The measured voltage (volts);

I: the source current (amperes);

d: the sample thickness (cm);

Based on a formula (I-2), we deduce the following:

$$R_S = \frac{\pi}{\ln 2} \cdot \frac{V}{I} = 4 \cdot 53 \frac{V}{I} \qquad \text{(II.12)}$$

II.4 Conclusion

In this chapter we have presented the deposition ways of the thin layers these ways are divided into two parts: physical and chemical such as spray pyrolysis which is the spot of our study and some different analysis technique used in our characterization study, namely X-ray diffraction (XRD), Spectroscopy (UV-Vis), four-point resistivity and weight difference methods were present.

Chapter three:

Results and discussions

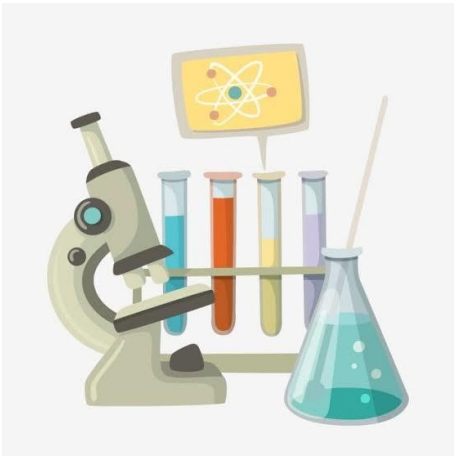

III.1.Part A: Experimental Work

III.1. 1.Experimental conditions:

✓ The Substrate temperature: 420 °C.

✓ Spout-Substrate distance: 24 cm.

✓ The Quantity of the solution: 5 ml.

✓ The Deposit time: 20 - 25 min.

✓ Pressure: 2 bars.

III.1. 2.Experimental setups:

❖Calculate weights:

The weights were measured by sensitive electronic balance with four digits (10^4g) sensitivity figure III.1 .The appropriate weight of the materials $Ni(NO_3)_2.6H_2O$ and $CuCl_2.2H_2O$ were determined by using the following equation:

$$\mathbf{m = M \times C \times V} \qquad \text{(III.1)}$$

Where:

m: Mass Molar of the Powder (g).

M: Molar mass (mol).

C: The concentration (mol/L).

V: The volume of distilled water (L).

✓ Calculate weight(m) of Ni $(NO_3)_2.6H_2O$:

We prepare the solution by dissolving Nickel dinitrate hexahydrate with a concentration of 0.15 mol / l in a volume of 50 ml (Methanol + distilled water). The mass of Nickel dinitrate hexahydrate is calculated by the following relationship:

Which C = 0.15 mol / l and the volume V = 50 ml

For a mass m we have:

- $M_{Ni(NO3)2.6H2O}$= 290.806 g/mol
- m_{Ni}= 58.69 g/mol

$\mathbf{m}_{Ni(NO3)2.6H2O} = \mathbf{M \times C \times V}$

$\mathbf{m}_{Ni(NO3)2.6H2O}$ = 290.806×0.15×0.05= 2.181 g

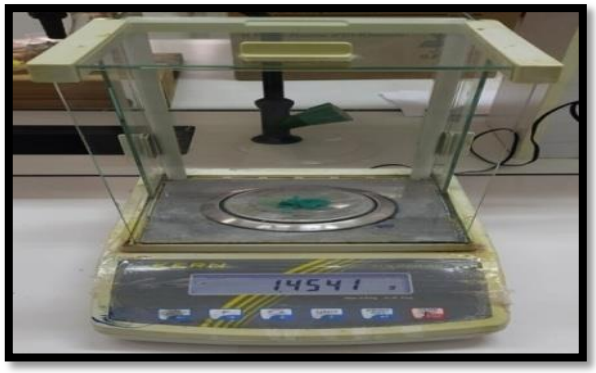

Figure III.1: Sensitive electronic balance with four digits (10^4g) sensitivity.

✓ **Calculate weight of Ni:**

$$m_{(\mathrm{Ni})} = \frac{m_{(\text{Nickel dinitrate hexahydrate})} * M_{(Ni)}}{M_{(\text{Nickel dinitrate hexahydrate})}} \quad \text{(III.2)}$$

$$m_{(Ni)} = \frac{2{,}181 * 58{,}69}{290{,}806} = 0{,}4402 \text{ g}$$

$$m_{Ni} = 0.4402 \text{ g}$$

✓ **Cupric chloride dihydrate doped:**

- $m_{(CuCl2,\ 2H2O)}$= 170,482 g/mol
- $m_{(Cu)}$= 63,55 g/mol

$$m_{Cu} = m_{Ni} \times 1\% \text{ doped}$$

$$m_{Cu} = 0.4402 \times 0.01$$

$$m_{Cu} = 0.0044 \text{ g}$$

✓ **Cupric chloride dihydrate doped for 1%:**

$$m_{(CuCl2,\ 2H2O)} = \frac{m_{Cu} \times M_{(CuCl2,2H2O)}}{M_{Cu}} \quad \text{(III.3)}$$

$$m_{(CuCl2,\ 2H2O)} = \frac{0.0044 \times 170.482}{63.55}$$

$$m_{(CuCl2,\ 2H2O)} = 0.0118 \text{ g}$$

✓ **Cupric chloride dihydrate doped for 0.5 %:**

$$m_{(CuCl2,\ 2H2O)} \times 0.5 = 0.0118 \times 0.5 = 0.0059 \text{ g} \quad \text{(III.4)}$$

To calculate the rest of masses for different doping percentage we are using the same method.

✓ **Calculate weight of $CuCl_2.2H_2O$:**

The different weight mass of the different doping percentage (0, 0.5, 1.5, 3 and 6) % are calculated and presented in the table III.1.

Table III.1: The weights of powder used in the preparation of the solution.

Doping percentage (%)	Weights (g)
Undoped	$m_{Ni\ (NO3)2.6H2O} = 2.181$
0.5	$m_{COCl2.6H2O} = 0.0059$
1.5	$m_{COCl2.6H2O} = 0.0177$
3	$m_{COCl2.6H2O} = 0.0354$
6	$m_{COCl2.6H2O} = 0.0708$

III.1.3.Preparation of solution:

- **$Ni(NO_3)_2.6H_2O$:** Green powder of Nickel Nitrate is the primary source of materials, with 2.181 g dissolved in 50 ml of distilled water at 50 °C with concentration of 0.15 (mol/L).

Product Specification

NICKEL (II) NITRATE (HEXAHYDRATE) AR

PRODUCT CODE	593745
SYNONYMS	[Nickel (II) nitrate hexahydrate]
C.I. NO.	--
CASR NO.	(13478-00-7)
ATOMIC OR MOLECULAR FORMULA	$Ni(NO_3)_2.6H_2O$
ATOMIC OR MOLECULAR WEIGHT	290.79
PROPERTIES	Melting point 55°C

$Ni(NO_3)_2.6H_2O$

PARAMETER	LIMIT
Description	Green crystals/crystalline powder.
Solubility	10% solution in water is bright and clear.
Minimum Assay (complexometric)	99.0%

Figure III.2: Profile of Ni $(NO_3)_2.6H_2O$ [66].

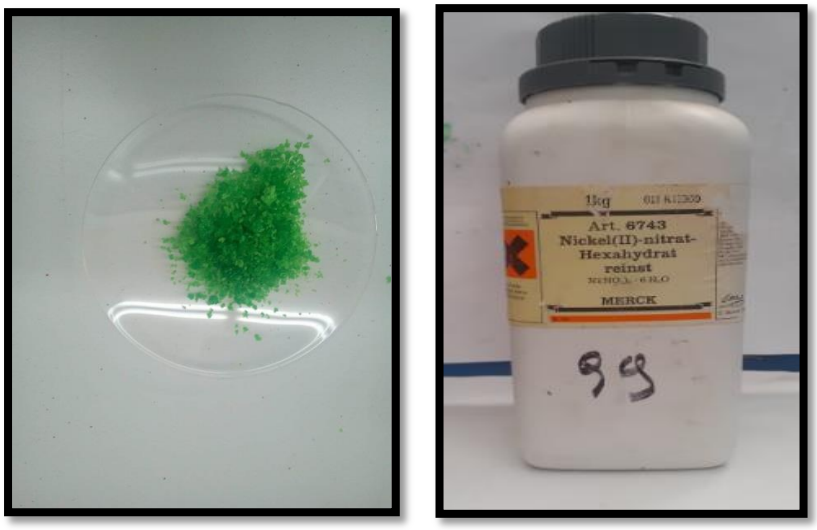

Figure III.3: Powder of Nickel Nitrate.

- **$CuCl_2.2H_2O$:** The solution was prepared by dissolving 2.181 g of Nickel Nitrate with the right weights of Copper Chloride. After dissolving each masse of varied doping percentage of ($CuCl_2$,$2H_2O$) (0.0059, 0.0177, 0.0354 and 0.0708 g) with Nickel Nitrate. We added 50 ml of distilled water for these solutions and then let stirred at 50 °C

1.1. Product identifier		
Product form	:	Substance
Trade name	:	Copper (II) chloride dihydrate AGR
EC no	:	231-210-2
CAS No	:	10125-13-0
REACH registration No	:	01-2119970306-36
Product code	:	CUCH-02A
Formula	:	CuCl2·2H2O
1.2. Relevant identified uses of the substance or mixture and uses advised against		
1.2.1. Relevant identified uses		
Main use category	:	Laboratory use

Figure III.4: Profile of $CuCl_2.2H_2O$ [7].

Figure III.5: Powder of Copper Chloride dihydrate.

❖The solution preparation steps are as follows:

- ✓ Added to 50 ml of distilled water, the necessary amount of Nickel Nitrate as well as the Copper Chloride**.**
- ✓ Mixing everything with average speed of rotation using (Magnetic Stirrer) tray heated at temperature of 50 °C in 60 minutes to make sure that no residues were left and to ensure the homogeneity of the resultant solution (figure III.6)**.**
- ✓ The resultant solution put it in glass bottle and kept to cool at the temperature of the room for 24 h (figure III.7)**.**

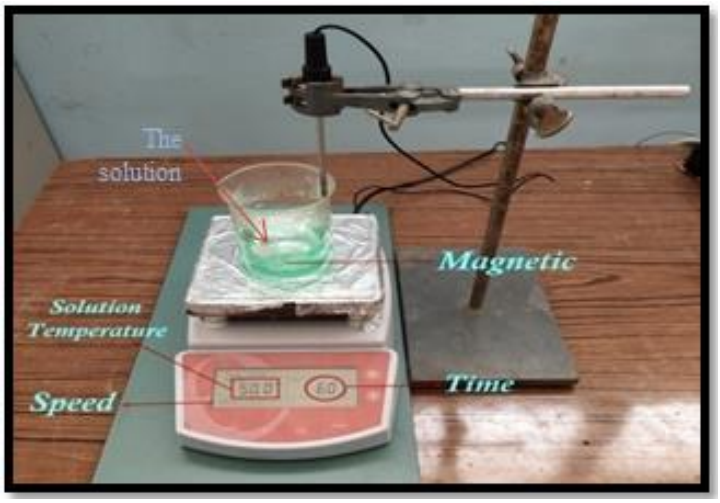

Figure III.6: (Magnetic stirrer) tray heated (University of Tebessa).

Figure III.7: Chemical Solution prepared.

This method of forming thin layers on glass substrates is done by the union of Nickel ions with the Oxygen ions present in the air of the furnace « case of non-doping».

$$\mathbf{2\ (Ni\ (NO_3)_2.6H_2O) \xrightarrow[420\ °C]{} 2Ni + 4NO_2 + O_2 + 12(H2O)} \qquad \text{(III.5)}$$

The Nickel ions and those of Copper are associated with Oxygen ions at a temperature of 420 °C. This solution is prepared with different percentages of Cu, as indicated in table III.2.

Table III.2: The volumetric ratios of the solutions used in the preparation of thin films.

Doping percentage (%)	**Solution of $Ni(NO_3)_2.6H_2O$**	**Solution of $CuCl_2.2H_2O$**
un doped	100	0
0.5	99.5	0.5
1.5	98.5	1.5
3	97	3
6	94	6

III.1.4.Preparation of substrates:

A/Choice of substrate

This choice allows us to carry out a good optical and electrical characterization of the layers; we used glass microscope slides with the dimensions of (25.4 x 76.2 mm²) and a thickness of 1-1.2 mm (figure III.8).

The substrates used are glass slides; the choice of glass is due to three reasons:

- It makes it possible to carry out a good optical characterization of the films which adapts well for their transparency.

- After deposition, the sample (substrate + layer) will undergo a cooling from the deposition temperature above 420 °C to ambient temperature (~ 25 °C) which causes compressibility of the two materials constituting the sample. In this case, they have very close expansion coefficients, which minimize the stresses. Note that an increase in the temperature of the substrate leads to an increase in stresses. This is linked to the compressive stress caused by the difference between the expansion coefficients of the substrate and of the material deposited :

  (α glass = 8.5×10^{-6} K^{-1}, α NiO = 7.93×10^{-6} K^{-1})

- Economic reasons [67].

Figure III.8: Type of glass substrates used.

B/Cleaning of substrates:

The cleaning of the substrate is very important because it has a great effect on the properties of the films and the step determines the qualities of adhesion and homogeneity of the deposited layers, The quality of the deposit and consequently that of the sample depends on the cleanliness and the state of the substrate, remove all traces of grease and dust and visually check that the substrate surface is free of scratches and flatness clear as crystal. These conditions are essential for the good adhesion of the deposit to the substrate, and for its uniformity (constant thickness).to do this, it is essential to go through the substrate cleaning process because the electrical characteristics are very sensitive to surface preparation techniques.

- The process can be summarized by the following steps:
- Cleaning with (20 ml HCL + 100 ml distilled water) for 5 min at room temperature:

« To remove any traces of grease and impurities attached to the surface of the substrate».

- Washing in a bi-distilled water bath for 5 min.
- Cleaning with (5 ml Methanol + 5 ml Acetone) for 5 min:

«This reacts with contamination such as grease and some oxides».

- Washing in a bi-distilled water bath.
- And finally, drying using an electrical oven and Josef paper.
- Avoid touching the surface of the substrate to avoid contamination.

C/Cuts & remarks of substrates:

The figure III.9 show the methods of cuts and remarks of the substrates to 3 section of (2.5× 2.5) Cm².

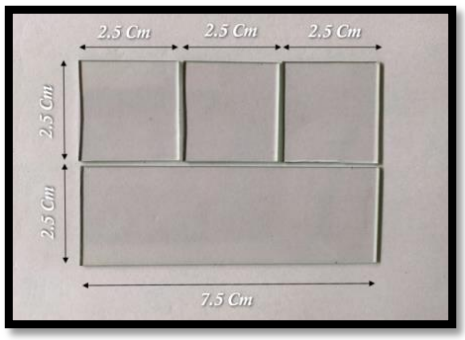

Figure III.9: The substrates cuts method.

III.1.5 chemical spray pyrolysis device:

- Figure III.10-11shows the chemical spray pyrolysis device used in the preset work.

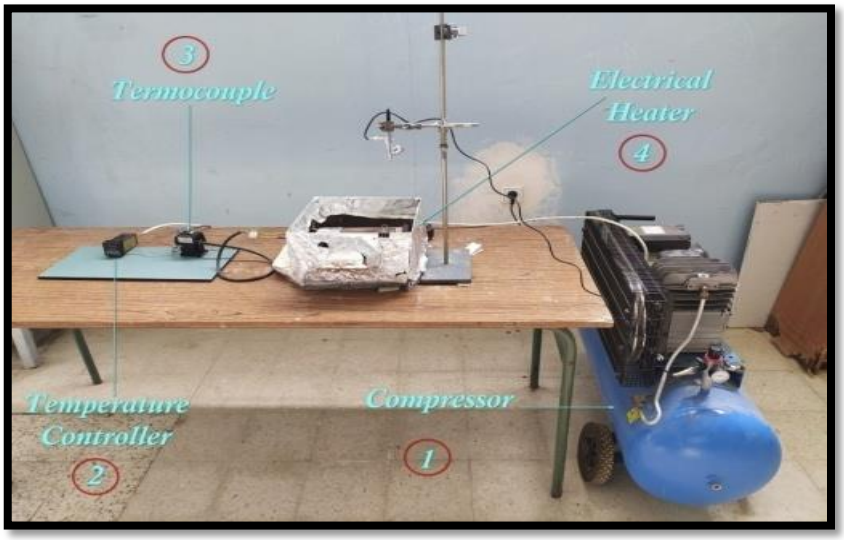

Figure III.10: Experimental device of the pyrolysis spray.

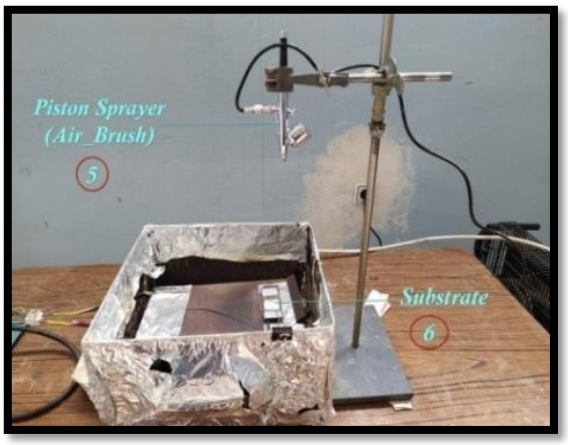

Figure III.11: Part of heating of pyrolysis spray device.

- The main elements of this assembly are:

1. Air compressor

Under a controllable pressure (P = 2 bar) the compressor pushes the pressurized air drop from glass bottle; this leads to make the solution flows from the capillary tube to the glass substrates, as soft spray.

2. Thermocouple

This includes a sensitive thermal wire; it is attached to the hot plate and joined to the digital temperature controller which fixes the temperature of the surface of the plate to the desired value.

4. Electrical heater

The heater is used for heating the plate on which the glass substrate is placed, to deposit the thin film. In this study the temperature used was 420± 20 ° C.

5. Airbrush

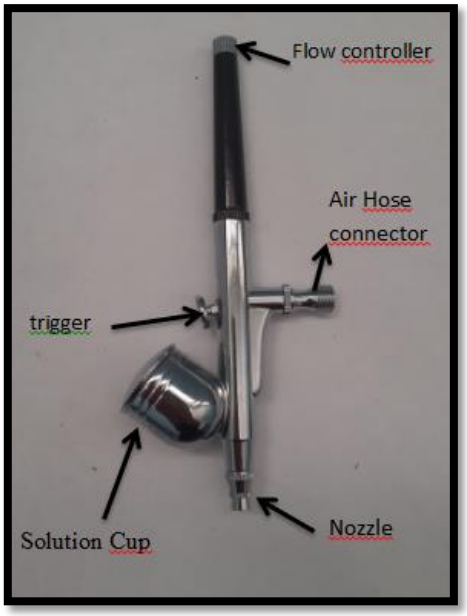

Figure III.12: Royal Max Airbrush Gun.

III.1.6.Parameters affects the films deposition:

a) Air pressure

In this study the air pressure was kept at (2 bar) to get uniform films the air pressure inside nozzle was adjusted to obtain fine atomizes in order to avoid the rapid decrease in substrate temperature which will cause the glass substrate to be broken.

b) Substrate temperature

One of the important parameters is substrate temperature it significant affect the homogeneity of the prepared films, because it is responsible for the variation of the crystal structure of the material that affects the physical properties of the materials.

c) Spraying rate

Sprayer rate might cause a significant decrease in substrate temperature and lead to substrate crush. This parameter affects the homogeneity and thickness of the prepared films. In this study the spraying rate of the films was kept at (5 ml/min) to ensure a good stoichiometry and obtain a homogenous film.

d) Spraying time

It is important to control the time period between every spraying operation, it should be uniform, and the spraying time period was 10 sec with 2 minutes wait between any two successive sprayings.

e) Distance « Nozzle from the substrate »

To obtain uniform film it is important to check the distance from the end of the capillary tube to the substrate is. In the present experiment the distance was fix it at 24 cm.

Different distance causes scattering of the atomized solution away from the substrate, also any decrease in this distance will cause the collection of solution drops in one spot and this will affect film homogeneity.

a) The drops size effect

The best deposition processes depend on the size of drops. The drops size effect on the preparation of obtains homogenous thin films. We have three Cases as we are showed in figure III.13 [68]**:**

Case A:

In this case, the drops size is large; therefore, the absorbed heat is not enough for solution evaporation. So, when the drop collides with the substrate it produces solid precipitate after solvent evaporation with a high decreasing rate in substrate temperature which causes the formation of inner potentials and leads to obtain a heterogeneous thin film and this affects the physical properties of the thin film.

Case B:

This represents the chemical spray pyrolysis operation, which gives the perfect properties for the thin film. In this case, the fine drops will evaporate in a short time before they reach the substrate, i.e. the particles reach the heated substrate as vapor phase, thus it can get enough heat to elevate its temperature, and therefore, the reaction on the substrate will take place.

Case C:

In this case, the drops are dried before they reach the substrate and become as powder on the substrate, which is distributed and condensed as smooth Grains on the substrate surface, it can easily be removed because its adhesion to the substrate is weak, this case happens when the spray distance is large.

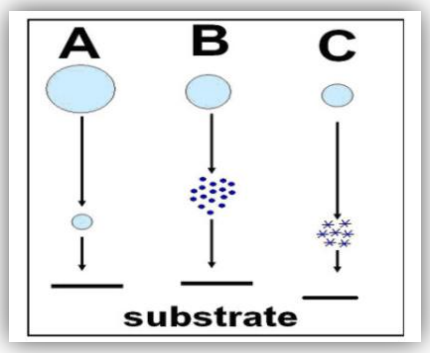

Figure III.13: The drops size effect [69].

III.2.Part B: Characterization techniques

III.2.1 Image of thin films prepared

Figure III.14 shows the photo image of Nickel-Copper Oxide thin films, of varied doping percentage (x = 0, 0.5, 1.5, 3 and 6 %). It is reported that the stoichiometrically correct NiO thin films are expected to have grey color; however, the non-doped NiO thin film deposited in the present study has black-grey color which can be attributed to non-stoichiometry of the deposited material. It can also be observed that the Cu-doped NiO thin films are accompanied by a color change from grey to black which we notes it in 6% Cu percentage . This change of color is attributed to the Copper doping percentage.

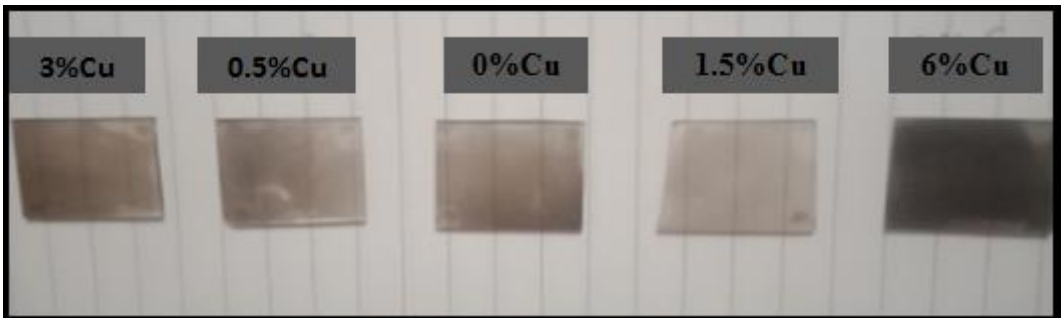

Figure III.14: Photo image of (Ni Cu x %) thin films, where x = 0, 0.5, 1.5, 3 and 6 % of copper doping.

III.2.2 Optic characteristic:

III.2.2.1 Transmittance spectrum

Figure III.20 shows the transmission spectra of the sprayed CNO thin films in the wavelength range of 200-1100 nm. It is observed that the transmission is about 50-70 % in the visible range. Which the maximum value is reached to 70 % for 1.5 % and decreases to the minimum 50 % in the infrared domain for 6 % of copper doping percentage.

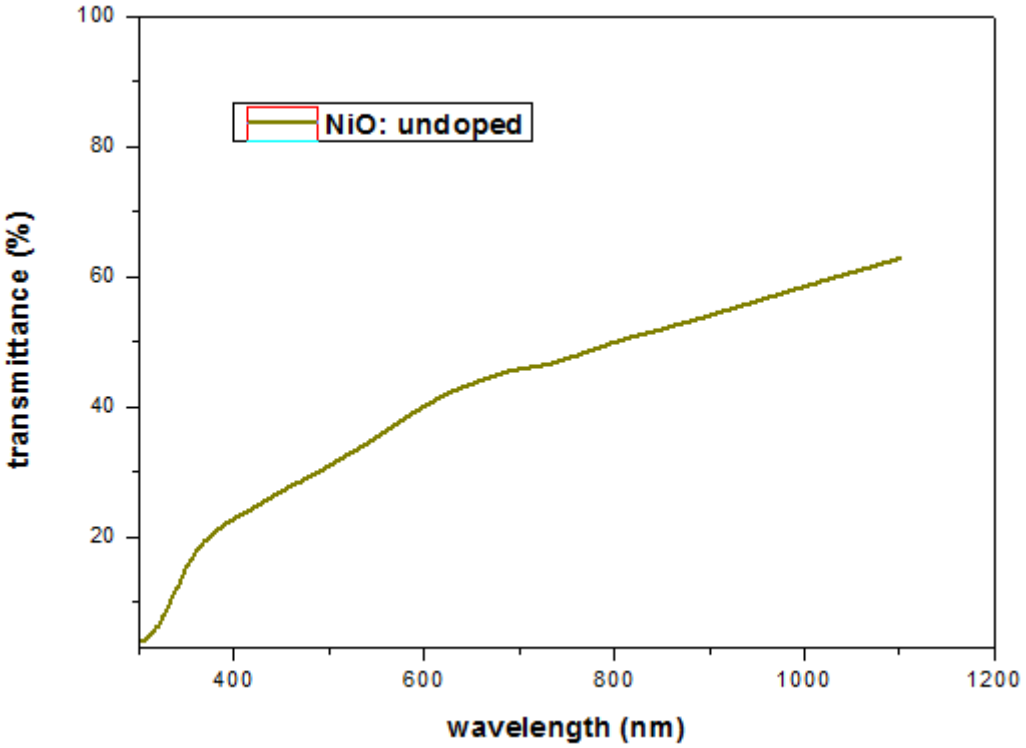

Figure III.15: Transmittance spectra for the undoped NiO.

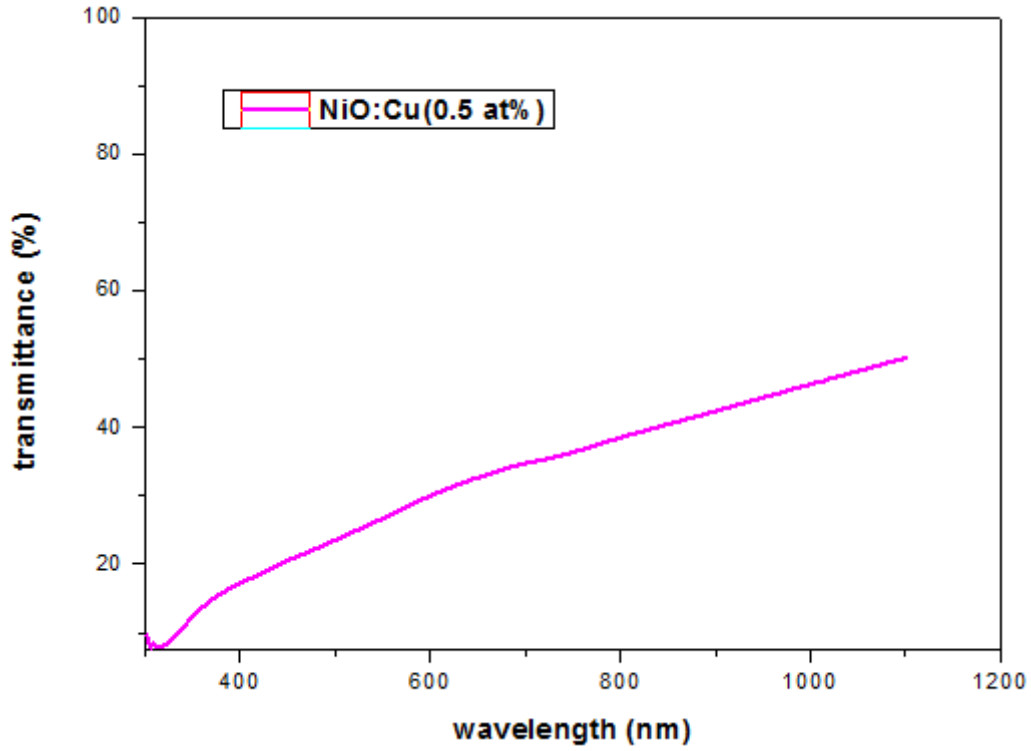

Figure III.16: Transmittance spectra for NiO doped 0.5 % Cu.

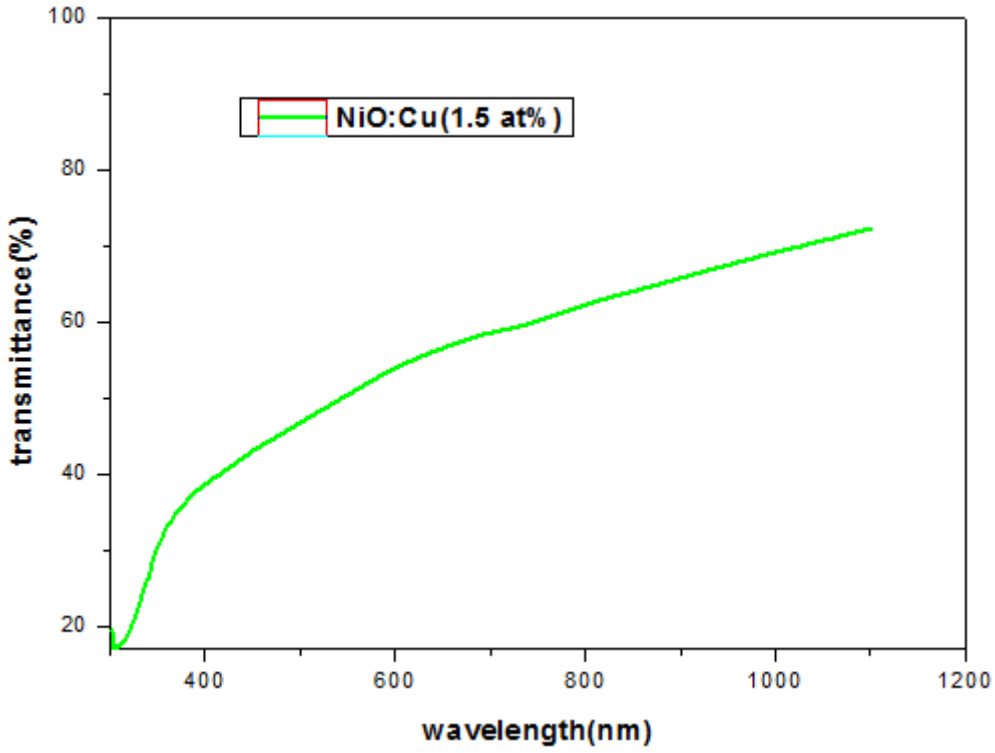

Figure III.17: Transmittance spectra for NiO doped 1.5 % Cu.

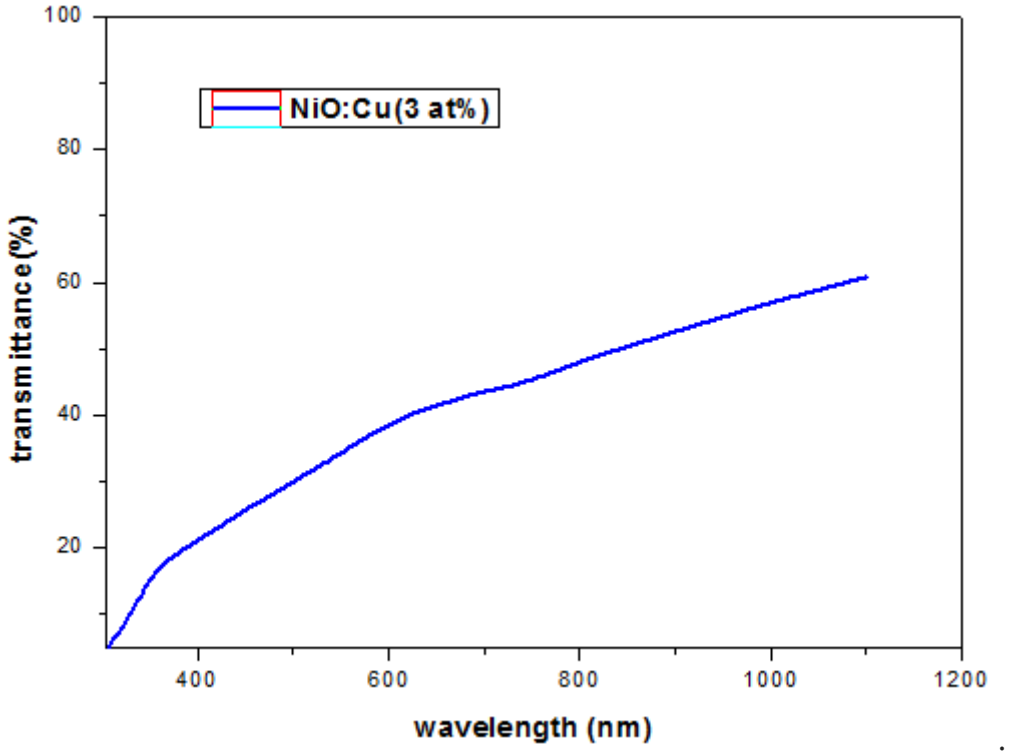

Figure III.18: Transmittance spectra for NiO doped 3 % Cu.

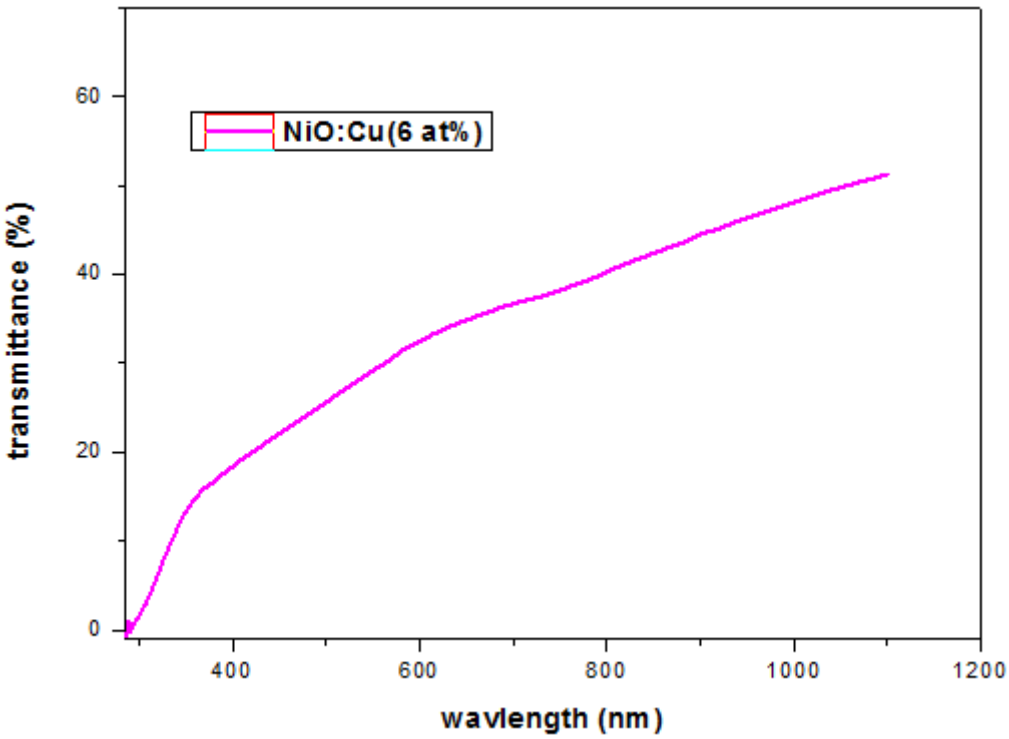

Figure III.19: Transmittance spectra for NiO doped 6 % Cu.

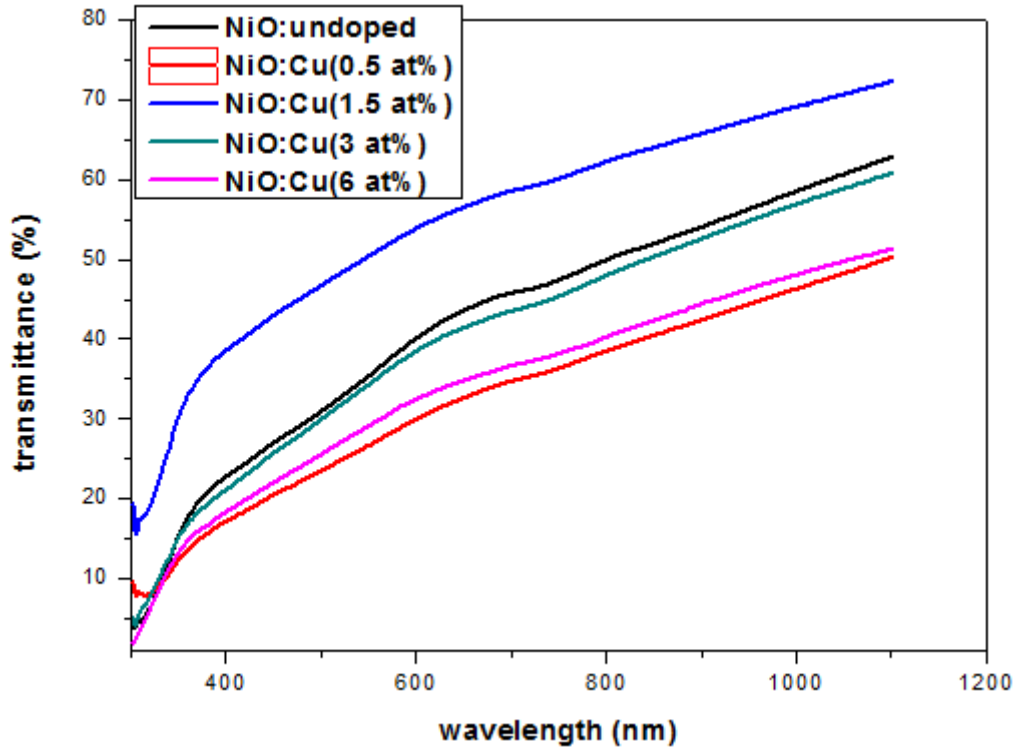

Figure III.20: Transmittance spectra versus wave length for undoped and Cu-doped (0.5, 1.5,3 and 6 %) NiO films prepared at 420 °C.

Table III.3: Transmittance values versus Cu doping percentage.

Cu (%)	0 %	0.5 %	1.5 %	3 %	6 %
Transmittance (%)	62.83	50.22	72.302	60.449	51.24

III.2.2.2 Gap energy (Eg)

From figure III.21, the band gap values are determined as a function of copper concentrations by extrapolating the straight line portion of the $(\alpha h\nu)^2$ versus (hν) variation to $(\alpha h\nu)^2 = 0$. The values were collected in the table III.3.

Which we notes that it is increase by increasing the percentage of copper between the range 3.0966 eV and 3.7479 eV

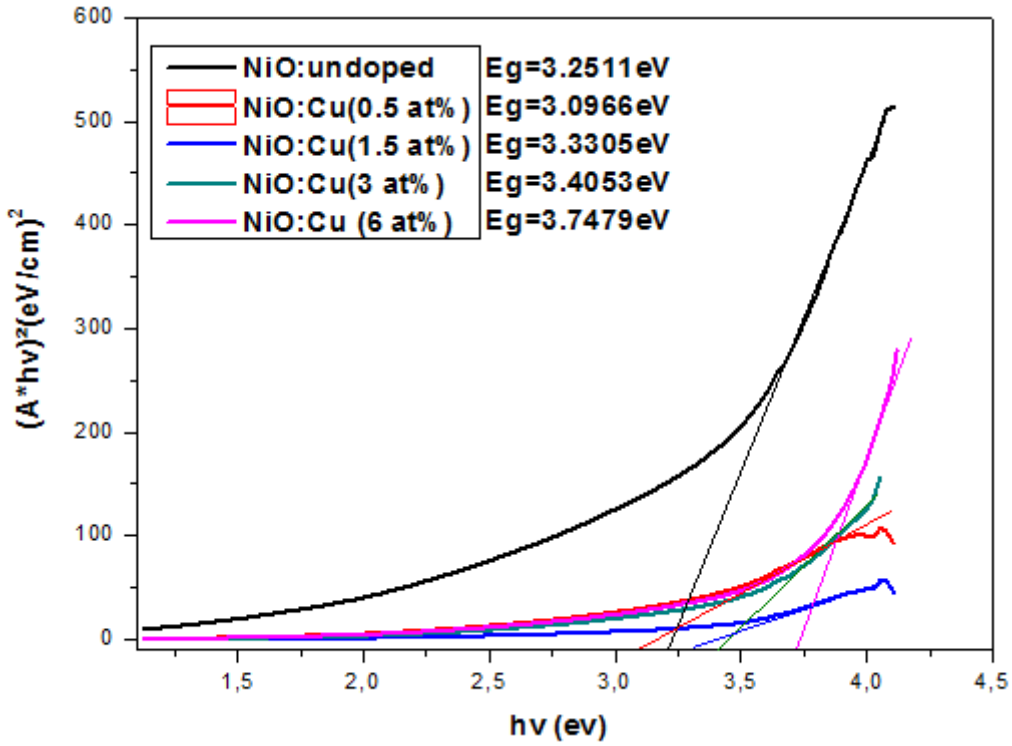

Figure III.21: Plots of $(Ah\nu)^2$ versus hν for NiO: Cu films with different values of copper doping percentage.

Table III.4: Gap energy values versus Cu doping percentage.

Cu (%)	0 %	0.5 %	1.5 %	3 %	6 %
Eg (eV)	3.2511	3.0966	3.3305	3.4053	3.7479

III.2.2.3 Urbach energy (Eu)

The Eu energy is determined using the plotting ln (A) vs. hv and fitting the linear part of the curve with a straight line .From the linear region of reciprocal of the slope give up the Eu value. The Eu values of the samples, which decreases in the case of crystallization at higher temperatures. Because Urbach energy of glassy semiconductors fundamentally defines the disorder level, crystallization and resulted order of this process decrease the Eu in value.

The results obtained shows that the Urbach energy decreases from 1779.2 meV at 0 % to 673.6 meV for 6 % Cu.

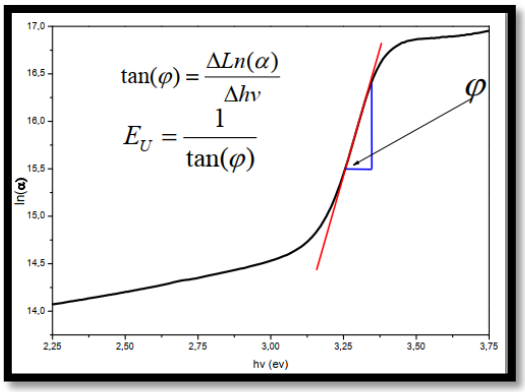

Figure III.22: Determination of Urbach energy of the layer [65].

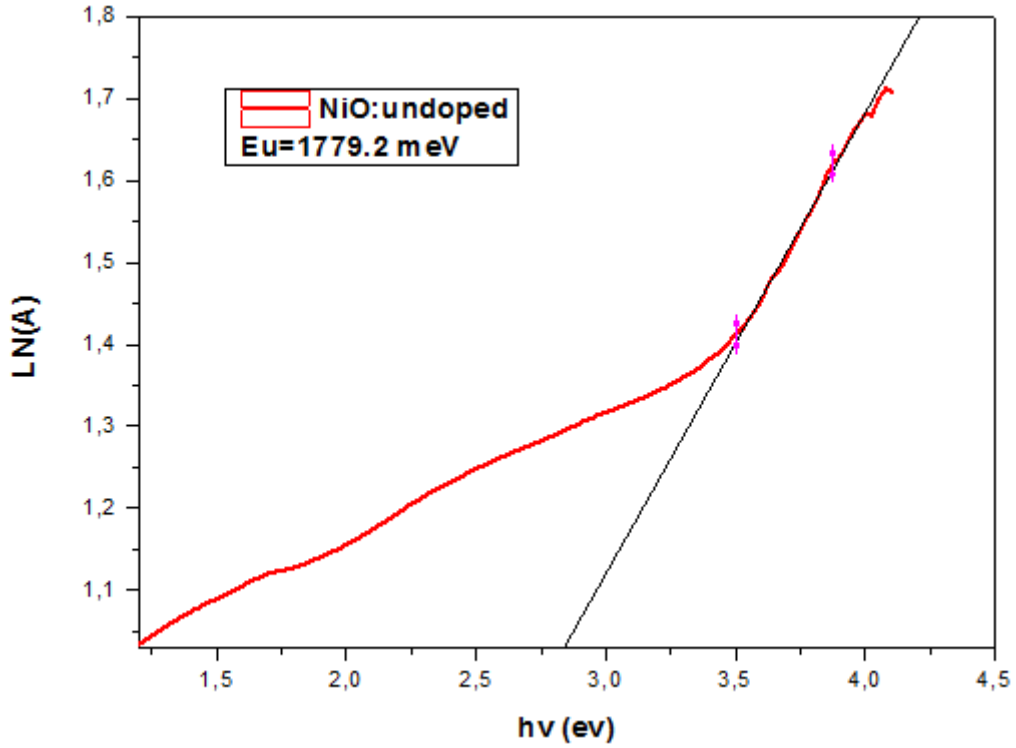

Figure III.23: Plot of Ln(A) versus *hv*(ev) for undoped NiO.

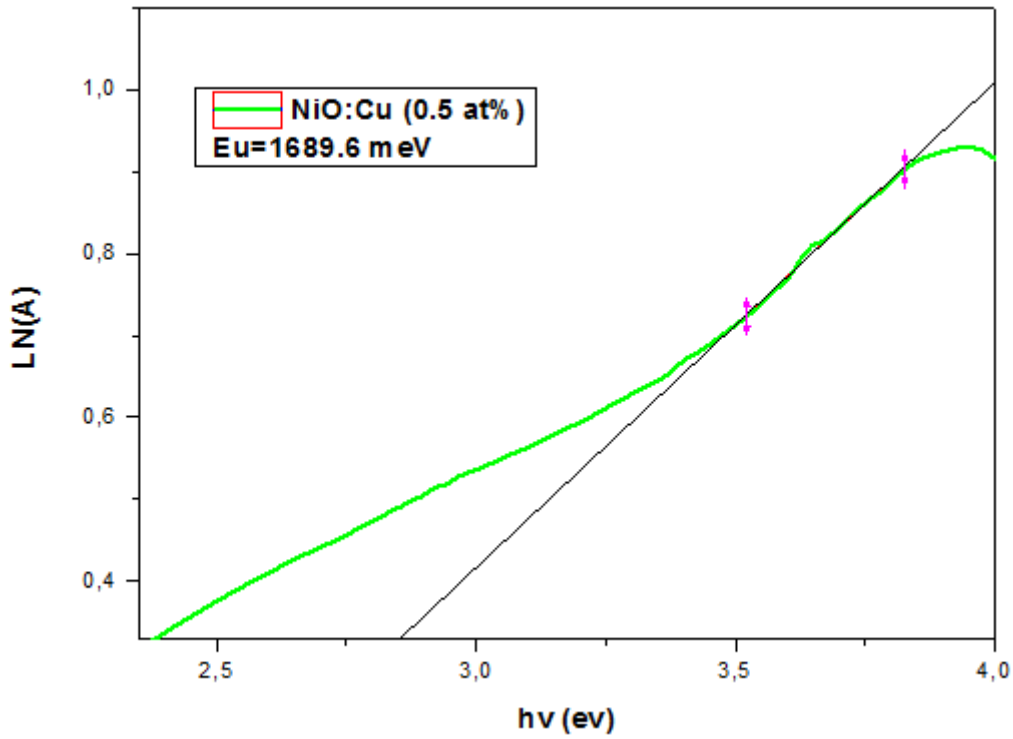

Figure III.24: Plot of Ln(A) versus *h*v(ev) for NiO 0.5% doped Cu.

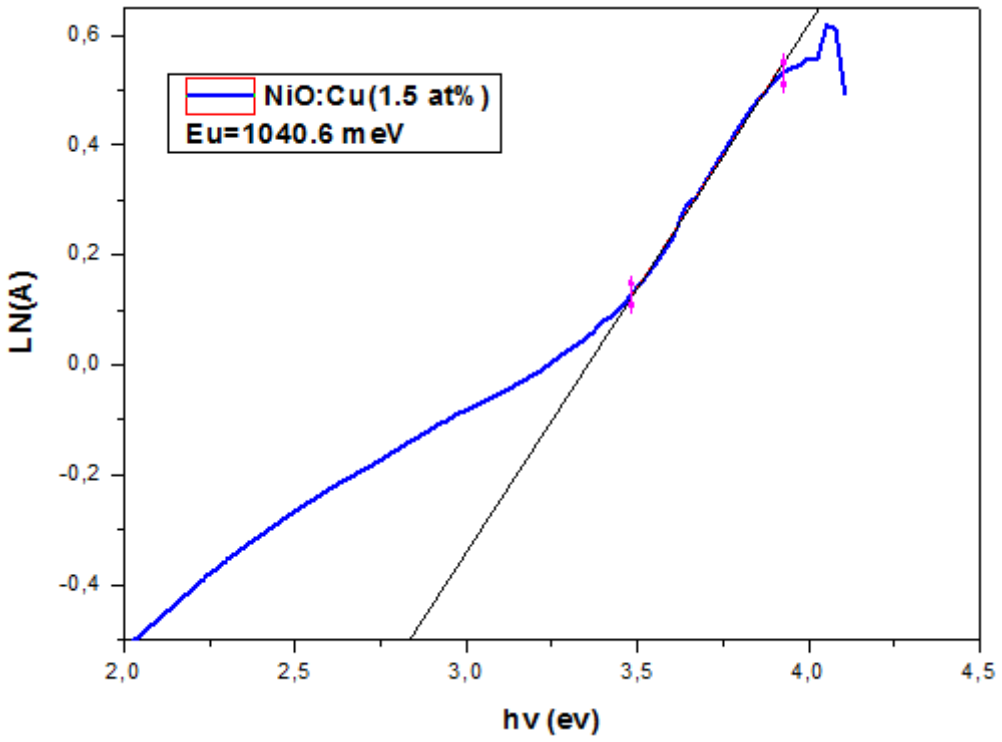

Figure III.25: Plot of Ln(A) versus *h*v(ev) for NiO 1.5 % doped Cu.

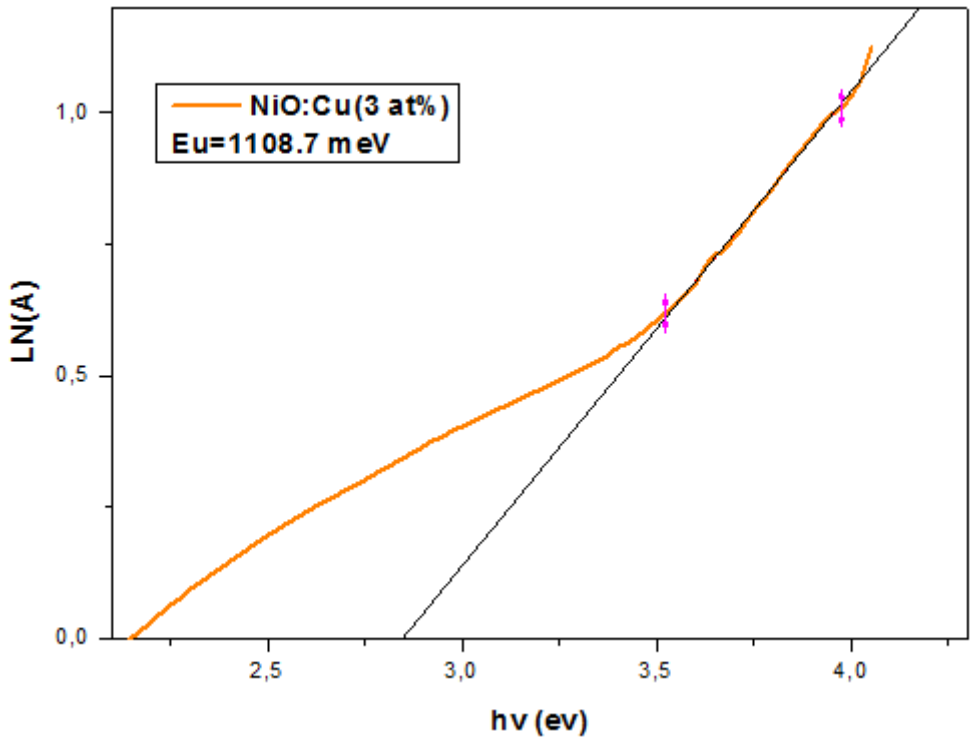

Figure III.26: Plot of Ln(A) versus *h*v(ev) for NiO 3 % doped Cu.

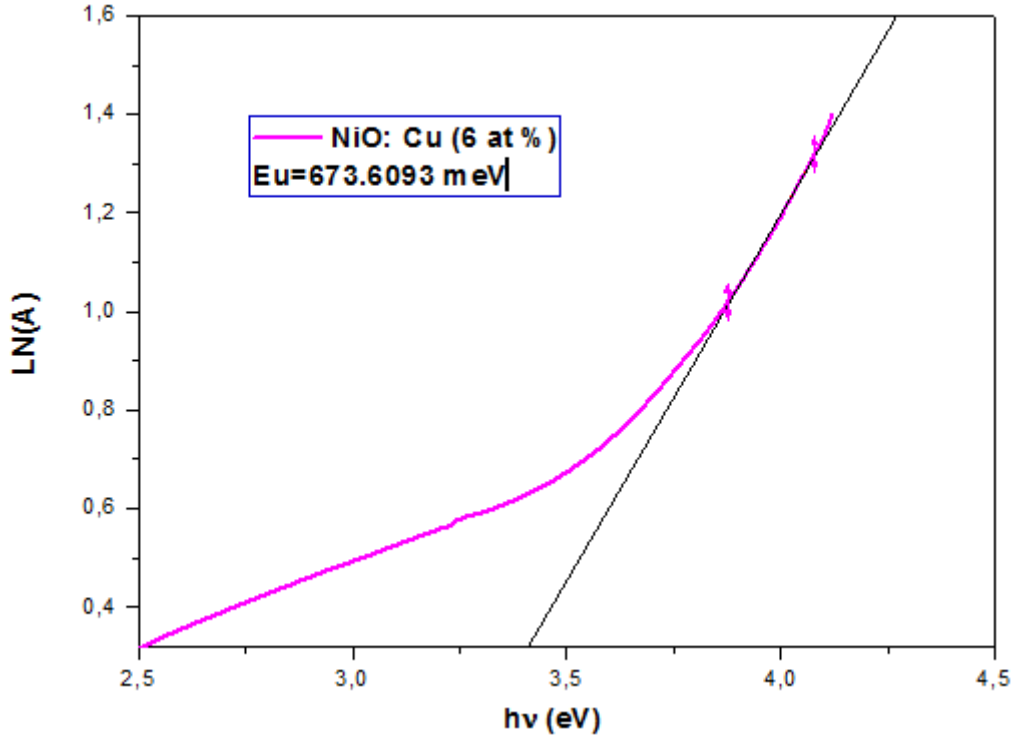

Figure III.27: Plot of Ln(A) versus *h*v(ev) for NiO 6 % doped Cu.

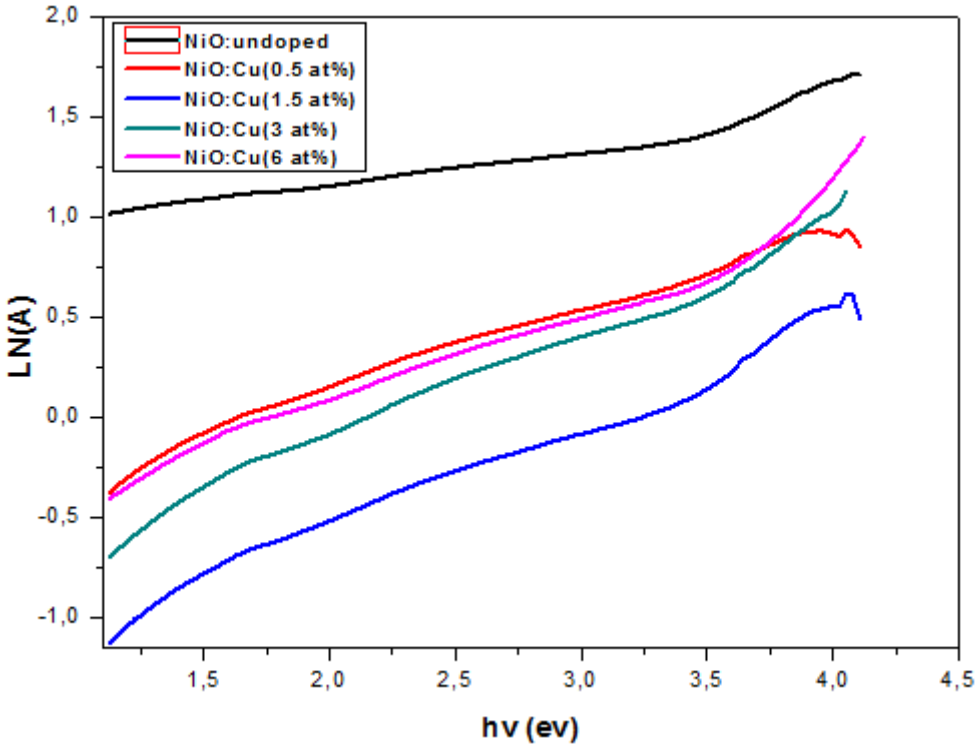

Figure III.28: Plots of Ln(A) versus hv for NiO: Cu films with different values of Copper.

Table III.5: Urbach energy values versus Cu doping percentage.

Cu (%)	0 %	0.5 %	1.5 %	3 %	6 %
Eu (meV)	1779.2	1689.6	1040.6	1108.7	673.6

Urbach energy decreases with increase of Cu-doping concentration..

III.2.1.4 Relation between Eg and Eu

We have noticed that Urbach energy values varied inversely proportional with the energy band gaps values versus Cu doping percentage of films (figure III.29).

.

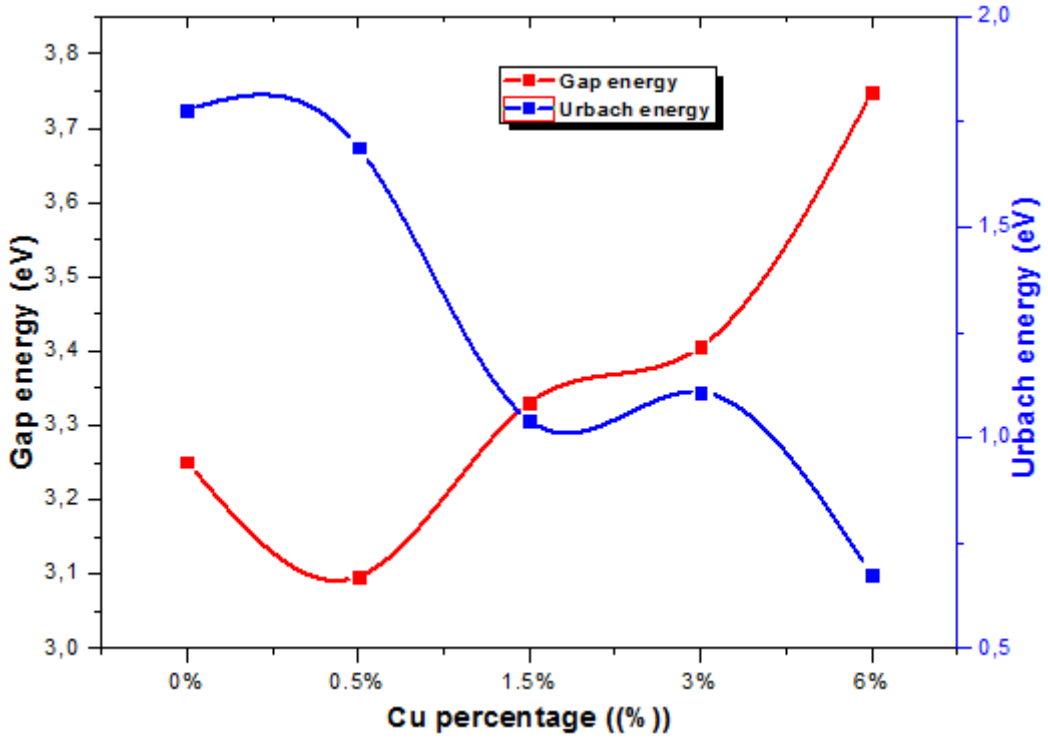

Figure III.29: Variation of the optical Gap and Urbach energy of NiO thin films versus Cu doping percentage.

III.2.1.5 Absorption

The optical absorption in thin films depends on thickness and wavelength and is a function of its structural properties.

The absorption spectra are the opposite of the transmittance spectra, the absorption coefficient decrease rapidly in the range 200 eV to 400 eV and increases slowly above 400 eV (visible region).

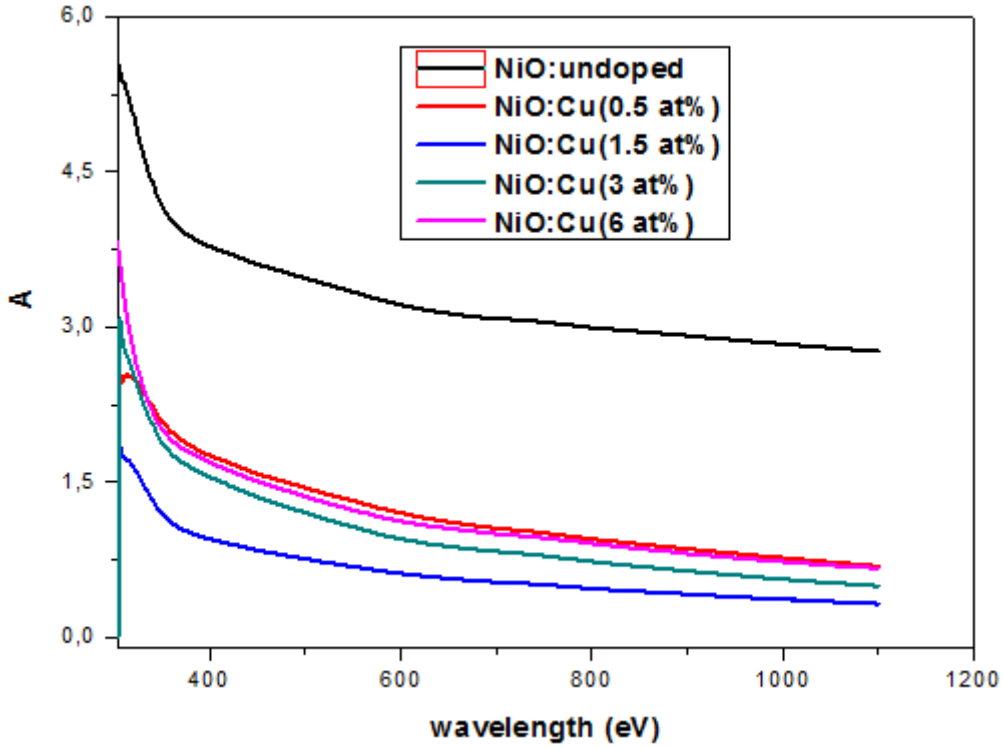

Figure III.30: The absorption spectra versus wave length for undoped and Cu-doped (0.5, 1.5,3 and 6%) NiO films prepared at 420 °C.

III.3 Conclusion:

In this study Nickel-Copper Oxide (Ni(1-x)CoxO) thin films, where x = 0, 0.5, 1.5,3 and 6 % were successfully deposited on glass substrate at (420 ºC) by chemical spray pyrolysis technique using Nickel and Copper chloride as the Ni and Cu source.

- The transmittance of Cu doped Nickel Oxide thin films increases rapidly as the wavelength increases in the range of (200-400) nm, and then increases slowly at higher wavelengths.
- The band gap increases as the Cu-concentration increases and the band gap values are in the range 3.09 eV to 3.74 eV.
- The Urbach energy decreases as the Cu-concentration increases and the Urbach energy values range are between 1779 meV and 673 meV.
- The absorption coefficient is the opposite of the transmittance spectra.

General conclusion

General Conclusion

The main goal of this work is the preparation and characterization of thin films based on NiO and doped oxide, and in order to achieve that, the whole experimental work has been done at the Laboratory of Materials at Larbi Tebessi University of Tebessa, Algeria.

So we started by preparing samples of thin layers of Nickel Oxide, which have been doped with different percentages of Copper (0.5, 1.5, 3, and 6 %), where we have deposited these layers on glass substrate at 420 ^{o}C by spray pyrolysis technique (SPT) to study the effect of doping of Nickel Oxide by Copper on the structural, optical and electrical properties. To characterize these samples, we have to use several techniques, such as, UV-Visible spectroscopy for optical characterization, the four-point method for electrical characterization and weight difference methods for thickness measurement.

The results collected from this study are:

The transmission and absorption spectra of the sprayed CNO thin films in the wavelength range of 200-1100 nm. It is observed that the transmission is increases rapidly as the wavelength increases in the range of (200-400) nm, and then increases slowly at higher wavelengths. Which the maximum Transmittance was reached above 72 % for 1.5 % of Cu doping percentage.

The band gap increases as the Cu-concentration increases and the band gap values range between 3.09 eV and 3.74 Ev, which are agreement with other research.

The Urbach energy decreases as the Cu-concentration increases and the Urbach energy values range between 1779 meV and 673 meV.

We have noticed that the absorption coefficient is the opposite of the transmittance spectra.

References

References

[1] R. Li and Hong Meng, "Organic Light-emitting Materials and Devices". CRC Press, USA, (2007).

[2] Dedova, Tatjana, PhD, "Chemical spray pyrolysis deposition of Zinc sulfide Thin Film and Zinc Oxide Nanostructured Layers", Volume 20, (2009).

[3] http://fr.wikipedia.org/wiki/thinfilms

[4] A.Jilani, M;Shaaban ,A.wahab and A.Hosny, Advance Deposition Techniques for Thin Film and Coating ,introduction and deposition techniques ,(2016).

[5] M. Boussafeur, Master thesis, Larbi Ben MHidi University Oum El-Bouaghi, (2012).

[6] A.berganer, thin film technology physics of thin films Vol. 138, No. 30, No. 32, (2010).

[7] Www.Google.com.

[8] http://fr.wikipedia.org/wiki/couche_mince.57.

[9] S.Senroy, "Characterization of copper oxide, titanium oxide and copper doped titanium oxide thin films prepared by spray pyrolysis technique", Doctoral Thesis, Bangladesh University, Bangladesh, (2016).

[10] D. W. Pashley, "The nucleation, growth, structure and epitaxy of thin surface films", Advances in Physics, Vol. 14, No. 55, 327-416,(1965).

[11] J. L. McCormick and J. W. Westwater, "Nucleation sites for dropwise condensation", Chemical Engineering Science, Vol. 20, No. 12, 1021-1036, (1965).

[12] http://fr.wikipedia.org/wiki/nickeloxide

[13] Y. Zhao, H. Wang, C. Wu, W. Li, F. Gao, and G. Wu, “Study on the electroluminescence properties of diodes based on n-ZnO / p-NiO / p-Si heterojunction,” Opt. Commun, pp. 3–6, (2014)

[14] J.G. Aiken, A.G. Jordan, Electrical transport properties of single crystal nickel oxide, Journal of Physics and Chemistry of Solids, 29 (1968) 21.53.

[15] I. Sta, M. Jlassi, M. Hajji, and H. Ezzaouia, “Structural, optical and electrical properties of undoped and Li-doped NiO thin films prepared by sol-gel spin coating method,” Thin Solid Films, vol. 555, pp. 131–137, (2014).

[16] M. Doudi, N. Talebian, The study of antibacterial properties of NiO thin film using Sol-gel Synthesis, Biological Forum – An International Journal, 127-131(2016).

[17] http://fr.wikipedia.org/wiki/cooper

[18] C. Tsay and S. Yu, “Optoelectronic characteristics of UV photodetectors based on sol – gel synthesized GZO semiconductor thin films,” J. Alloys Compd., vol. 596, pp. 145–150, (2014).

[19] M. Gratzel, Dye-sensitized solar cells, Journal of Photochemistry and Photobiology, 4 145-153, (2003).

[20] O. Fellahi, Élaboration de nanofils de silicium par gravure chimique assistée par un métal: caractérisation et application en photocatalyse hétérogène de l’oxyde de graphène, du chrome (VI) et de la rhodamine B, thèse de doctorat, Université Sétif 1, (2014).

[21] D. Chatterjee, S. Dasgupta, Visible light induced photocatalytic degradation of organic pollutants, J. Photochem. Photobiol C, 6, 186–205, (2005).

[22] A.B. Djurisic, Y.H. Leung, A.M. Ching, Strategies for improving the efficiency of semiconductor metal oxide photocatalysis, Mater Horizons 1 400-410, (2014).

[23] A. Kumar, synthesis, characterization and application of bare and zinc doped nickel oxide nanoparticles, master of philosophy in chemistry, Shoolini University, 2013.

[24] Md. Tamez Uddin, Metal Oxide Heterostructures for Efficient Photocatalysts, Technical University of Darmstadt- Germany, thèse de doctorat, (2013).

[25] Fujishima, Akira, and Kenichi Honda. "Electrochemical photocatalysis of water at a semiconductor electrode." Nature, vol. 238. 5358, pp. 37, (1972).

[26] G.G. Bessegato, T. T. Guaraldo, J. F. Brito, M. F. Brugnera, and M. V. B. Zanoni. "Achievements and trends in photoelectrocatalysis: from environmental to energy applications," Electrocatalysis, vol. 6. 5, pp. 415-441, (2015).

[27] L. D. Smith, "Thin-Film Deposition Principles & Practice", McGraw-Hill: New York, (1995), pp.1-7.

[28] Z. Acosta, R.E, Romankiw, L.T, VonGutfeld, R. J, "Sol Thin Films", 95 (1982),131.

[29] L. D. Smith, "Thin-Film Deposition Principles & Practice", McGraw-Hill: New York, pp.1-7, (1995).

[30] K. Gelin; A. Roos; F. Geotti-Bianchini; P. v. Nijnatten, "Optical Materials", 27. (4), 705-712,(2005).

[31] R. Behrisch, "Sputtering by Particle Bombardment", Springer, Berlin (1981).

[32] Z. Acosta, R.E, Romankiw, L.T, VonGutfeld, R. J, "Sol Thin Films", 95 (1982), 131.

[33] K. L. Chopra, "Thin Film Phenomena", McGraw Hill, New York (1969).

[34] B. A. Movchan and A. V. Demchishin, "Study of the Structure and Properties of Dioxide thin, Fiz. Met. Metalloved", Vol. 28, 83-90, (1969).

[35] L. B. FREUND, S. SURESH, "Thin Film Materials Stress ", Defect Formation andSurface Evolution Cambridge University, (2003).

[36] J. R. Creighton and P. Ho**,**"Introduction to Chemical Vapor Deposition (CVD) ", Sandia National Laboratories P.O. Box 5800, MS0601 Albuquerque, NM 87185-0601, (2001).

[37] K. L. Chopra, "Thin Film Phenomena", McGraw Hill, New York (1969).

[38] P. Kirk and R Pillar, "The deformation response of sol-gel-derived thin films Mater". Sci, Vol. 34, 16, 3967-3975, (1999).

[39] A. Kopp Alves and al**.,**"Novel Synthesis and Characterization of Nanostructured Materials", Engineering Materials, DOI: 10.1007/978-3-642-41275-2, Springer-Verlag Berlin Heidelberg (2013).

[40] D. Perednis, "Thin film deposition by spray pyrolysis and the application in solide oxide fuel cells", Ph.D. Thesis, Swiss Federal Institute of Technology Zurich (2003).

[41] K. Choy, L. Su. B**,** "Growth behavior and microstructure of CdS thin films deposited by an electrostatic spray assisted vapor deposition (ESAVD) process", Thin Solid Films 388, 9–14 (2001).

[42] S.P.S. Arya and H.E. Hintermann, Thin Solid Films, 193(1–2), 841 (1990).

[43] M.GHOUGALI, Elaboration and characterization of nanostructuring NiO thin films for gas sensing applications, thesis of Doctorate, p13,(2019).

[44] L. Filipovic et al, "Methods of simulating thin film deposition using spray pyrolysis techniques", Microelectronic Engineering, Vol. 117, (2014), 57-66.

[45] Filipovic, Lado, et al. "Modeling spray pyrolysis deposition." Proceedings of the world congress on engineering. Vol. 2. (2013).

[46] Malik, Oleksandr, Francisco Javier De La Hidalga-Wade, and Raquel Ramírez Amador. "Spray Pyrolysis Processing for Optoelectronic Applications." Pyrolysis (2017): 197

[47] Kelly, A. J. "Charge injection electrostatic atomizer modeling." Aerosol Science and Technology 12.3 (1990): 526-537.

[48] D. Perednis and L. J. Gauckler, "Thin film deposition using spray pyrolysis", Journal of Electroceramics, Vol. 14, (2005), 103-111.

[49] L. Filipovic, Mem er, S. Sel erherr, G. C. Mutinati, E. Brunet, S. Steinhauer, . K ock, J. Teva, J. Kraft, J. Siegert, F. Schrank, C. Gspan and W. Grogge, "A Method for simulating spray pyrolysis deposition in the level set framework", Engineering Letters, Vol. 21, No. 4, (2013), 1-17.

[50] L. Filipovic, S. Sel erherr, G. C. Mutinati, E. Brunet, S. Steinhauer, . K ock, J. Teva, J. Kraft, J. Siegert and F. Schrank, "Modeling spray pyrolysis deposition", Proceedings of the World Congress on Engineering, Vol. 2,No. 3-5, (2013), 1-6.

[51] D. BEKKAR, Elaboration and optimization of Iron Oxide thin films deposited via spray pyrolysis. Applications in water treatment, thesis of doctorate, p33, 34, (2020).

[52] L. Filipovic et al, "Methods of simulating thin film deposition using spray pyrolysis techniques", Microelectronic Engineering, Vol. 117, (2014), 57-66.

[53] M. GHOUGALI, Elaboration and characterization of nanostructuring NiO thin films for gas sensing applications, thesis of doctorate, p20,21, (2019).

[54] A. Kumar, synthesis, characterization and application of bare and zinc doped nickel oxide nanoparticles, master of philosophy in chemistry, Shoolini University, (2013).

[55] A. Guinier, “X-ray Diffraction “, Freeman, San Francisco (1963).

[56] B. D. Cullity, “Elements of X-ray Diffraction”, Addison Wesley, Massachusetts (1956).

[57] A. Rahdar, M. Aliahmadb and Y. Azizi, "NiO Nanoparticles: Synthesis and Characterization", Journal of Nanostructures, Vol. 5, (2015), 145-151.

[58] A J. Ragina, Preparation and characterization of tin based semiconducting thin films, PhD thesis, Kannur University, (2012).

[59] JCPDS cards of NiO (Joint Committee on Powder Diffraction Standards).

[60] S A. Vanalakar, chemical synthesis of cds, ZnO and CdS sensitized ZnO thin films and their characterization for photo-electrochemical solar cells, PhD thesis, Shivaji University, Kolhapur, (2010).

[61] P. Sharma, an optical study of chalcogenide glasses using Uv-Visible-Nir

spectroscopy, PhD thesis, Jaypee University, (2015).

[62] Ikhmayies, S. J., & Ahmad-Bitar, R. N. (2013). A study of the optical bandgap energy and Urbach tail of spray-deposited CdS: In thin films. Journal of Materials Research and Technology, 2(3), 221-227.

[63] F. Urbach, The long-wavelength edge of photographic sensitivity and of the electronic absorption of solids. Physical Review, 92(5), (1953).

[64] Schroder, K. Dieter, "Semiconductor Material and Device Characterization", John Wiley & Sons, Inc, (1998).

[65] A. Benhaoua, A. Rahal , B. Benhaoua, M. Jlassi, "Effect of fluorine doping on the structural, optical and electrical properties of SnO2 thin films prepared by spray ultrasonic", Vol. 70, p. 61-69, (2014).

[66] JCPDS cards of NiO (Joint Committee on Powder Diffraction Standards).

[67] S A. Vanalakar, chemical synthesis of cds, ZnO and CdS sensitized ZnO thin films and their characterization for photo-electrochemical solar cells, PhD thesis, Shivaji University, Kolhapur, (2010).

[68] M. Amer Hassan, The effect of the annealing and annealing processes on some physical properties of the Cu2S film prepared by the method of pyrolysis, Master Thesis, University of Technology, Department of Applied Sciences (2002).

[69] A. Mahjoub, course in characterization techniques.

ملخص

في هذا العمل أعددنا أغشية رقيقة من أكسيد النيكل غير المشبع والمغلف بالنيكل من نترات النيكل المجففة Ni) (NO3) 2.6H2O)، كلوريد النحاس (CuCl2.2H2O) بتركيزات مختلفة من النحاس (0٪ ، 0.5 ٪ ، 1.5 ٪ ، 3 ٪ و 6 ٪) ، تم تثبيت المعلمات الأخرى مثل مولارية المحلول (0.15 مول / لتر) ، ودرجة حرارة الركيزة (T = 420 درجة مئوية) ، ووقت الترسيب (25 دقيقة) ، و مسافة الفوهة - الركيزة (24 سم) ، والرش بالضغط (2 بار), الرواسب المصنوعة في الركيزة بواسطة الانحلال الحراري بالرش الكيميائي. تم تحليل الأفلام التي تم الحصول عليها من خلال تقنيات توصيف مختلفة.

النتائج التي تحصلنا عليها كانت كالتالي:

- نفاذية الأغشية الرقيقة لأكسيد النيكل المشبع بالنحاس تزداد بسرعة كلما زاد الطول الموجي في نطاق (200-400) نانومتر ، ثم تزداد ببطء عند الأطوال الموجية الأعلى.
- تزداد فجوة النطاق مع زيادة تركيز النحاس وتكون قيم فجوة النطاق في النطاق 3.09 الكتروفولت إلى 3.74 الكتروفولت.
- تنخفض طاقة Urbach مع زيادة تركيز النحاس وتتراوح قيم طاقة Urbach بين 1779 meV و 673 meV.
- معامل الامتصاص هو عكس أطياف النفاذية.

الكلمات المفتاحية: الطبقات الرقيقة ، أكسيد النيكل (NiO) ، اعادة تطعيم ، رذاذ الانحلال الحراري ، النفاذية، الامتصاص.

Abstract

In this work , we have prepared thin films of undoped and cu-doped nickel oxide from nickel nitrate dehydrate ($Ni(NO_3)_2.6H_2O$**),** chloride of copper ($CuCl_2.2H_2O$) at different concentrations of copper (0, 0.5, 1.5, 3 and 6 %), other parameters was fixed such us the molarity of solution (0.15 mol/l), the temperature of substrate (T=420 °C), the deposition time (25 min), the nozzle-substrate distance (24 cm), and the pressure spraying (2 bar). The deposit made in substrate glass by chemical spray pyrolysis, the films obtained were analyzed by various characterization techniques.

The results we have obtained were:

- The transmittance of Cu doped Nickel Oxide thin films increases rapidly as the wavelength increases in the range of (200-400) nm, and then increases slowly at higher wavelengths.
- The band gap increases as the Cu-concentration increases and the band gap values are in the range 3.09 eV to 3.74 eV.
- The Urbach energy decreases as the Cu-concentration increases and the Urbach energy values range are between 1779 meV and 673 meV.
- The absorption coefficient is the opposite of the transmittance spectra.

Key words: thin films, nickel oxide (NiO), cu-doping, pyrolysis spray, transmittance, absorption

Résumé

Dans ce travail, nous avons préparé des couches minces d'oxyde de nickel non dopé et dopé au cuivre à partir de nitrate de nickel déshydraté ($Ni(NO_3)_2.6H_2O$), de chlorure de cuivre ($CuCl_2.2H_2O$) à différentes concentrations de cuivre (0, 0,5, 1,5, 3 et 6 %), d'autres paramètres ont été fixés tels que la molarité de la solution (0,15 mol/l), la température du substrat (T=420 °C), le temps de dépôt (25 min), le distance buse-substrat (24 cm), et la pulvérisation sous pression (2 bars). Les films obtenus ont été analysés par différentes techniques de caractérisation.

Les résultats que nous avons obtenus sont :

- La transmittance des films minces d'oxyde de nickel dopé au Cu augmente rapidement à mesure que la longueur d'onde augmente dans la plage de (200-400) nm, puis augmente lentement à des longueurs d'onde plus élevées.
- La bande interdite augmente à mesure que la concentration en Cu augmente et les valeurs de la bande interdite sont comprises entre 3,09 eV et 3,74 eV.
- L'énergie d'Urbach diminue à mesure que la concentration en Cu augmente et la plage des valeurs d'énergie d'Urbach se situe entre 1779 meV et 673 meV.
- Le coefficient d'absorption est l'opposé des spectres de transmittance.

Mots clés : couches minces, oxyde de nickel (NiO), dopage au cuivre, spray pyrolyse, , transmittance, absorption.